

SEISMICITY AND EARTHQUAKE HAZARD IN GIPPSLAND, VICTORIA

AMY BROWN⁽¹⁾, TREVOR ALLEN⁽²⁾ AND GARY GIBSON⁽¹⁾
SEISMOLOGY RESEARCH CENTRE⁽¹⁾ AND MONASH UNIVERSITY⁽²⁾

AUTHORS:

Amy Brown studied geological engineering at RMIT and has been working in earthquake hazard analysis at the Seismology Research Centre for several years. Amy is currently completing a Masters degree in Australian earthquake hazard and was awarded an AEES Scholarship in 2000.

Trevor Allen is a PhD student at the Department of Earth Sciences, Monash University, Melbourne. He is currently developing methods to investigate source parameters of small local earthquakes.

Gary Gibson has worked at the Seismology Research Centre since its inception in 1976 and at Phillip Institute of Technology and RMIT University since 1968. His interests lie in observational seismology and its practical applications.

ABSTRACT:

The Gippsland area east of Melbourne is one of the most seismically active areas in southeastern Australia. It is a geologically complex area with many faults identified using surface geology and topographical information. The region also hosts several large power stations and water storage dams.

Many of the known faults in Gippsland are located within the Strzelecki Ranges where faulting has continued from the mid Miocene to the present. The current stress is northwest to southeast compression, producing horst and graben structures by reverse faults striking northeast to southwest. Within the Strzelecki Ranges there are several faults that are of sufficient length to produce earthquakes larger than magnitude 7.

In the past, the identification of particular faults from seismicity data in Gippsland has not been possible, due to the high uncertainties in the earthquake locations.

A temporary network of seven seismographs was installed in the Strzelecki Ranges for a one year period to accurately locate earthquakes. Using locations and focal mechanisms to gain a 3-dimensional picture of the activity, it was possible to improve our understanding of both the faulting process and the nature of earthquake hazard in Gippsland.

1. INTRODUCTION

The Gippsland region is an important area within Victoria as it houses the majority of the state's power generation facilities and several large dams. Gippsland is also one of the most seismically active areas in southeastern Australia. There are many geologically defined faults in the area of sufficient length to produce an earthquake larger than magnitude 7. Gippsland is a region that has significant earthquake vulnerability.

The key to future estimates of earthquake hazard is in gaining a better understanding of the earthquake mechanisms through identification and quantification of active faults.

From August 2000 to September 2001 a dense seismograph network was operated in Gippsland to accurately locate earthquakes, and to provide a better understanding of the seismicity in the area. The network was located within the Strzelecki Ranges, southwest Gippsland. The Ranges consist of several fault bounded blocks with smaller internal faults. All of the faults identified in the Strzelecki Ranges have been geologically defined.

The original aim of the project was to use the accurately located earthquakes to delineate active faulting in the region. However, the level of activity was not sufficient to clearly identify any particular fault. The network did provide good depth constraints on the larger events, showing both shallow and deep activity from 3 to 20 km. The spread of activity over a wide depth range suggests that both the larger boundary faults and the smaller internal faults are active.

2. SEISMICITY IN GIPPSLAND

Gippsland is one of the most seismically active regions in southeastern Australia. Much of the earthquake activity in Gippsland is concentrated in the Strzelecki Ranges (Figure 1). The Ranges consist of several fault bounded blocks with smaller internal faults. The Narracan and Balook Blocks were uplifted during northwest to southeast compression in the Miocene along reverse faults (Douglas, 1988). The area is still undergoing compression and uplift. The Tarwin Valley forms the graben between the two blocks (Figure 2).

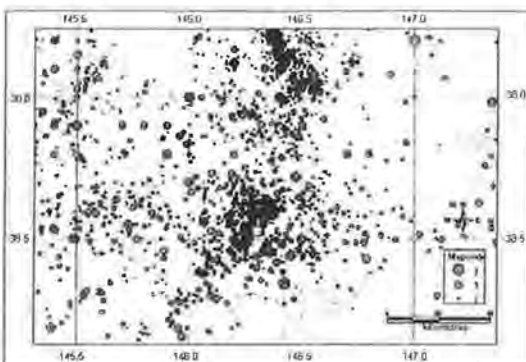


Figure 1: Seismicity of Gippsland

The uncertainties of most of the earthquakes located before August 2000 in the Strzelecki Ranges were too large to delineate active faults, although it was thought that most of the activity in the Tarwin Valley was occurring on the Yarragon or Yarram Faults (bounding faults of the Narracan and Balook blocks respectively).

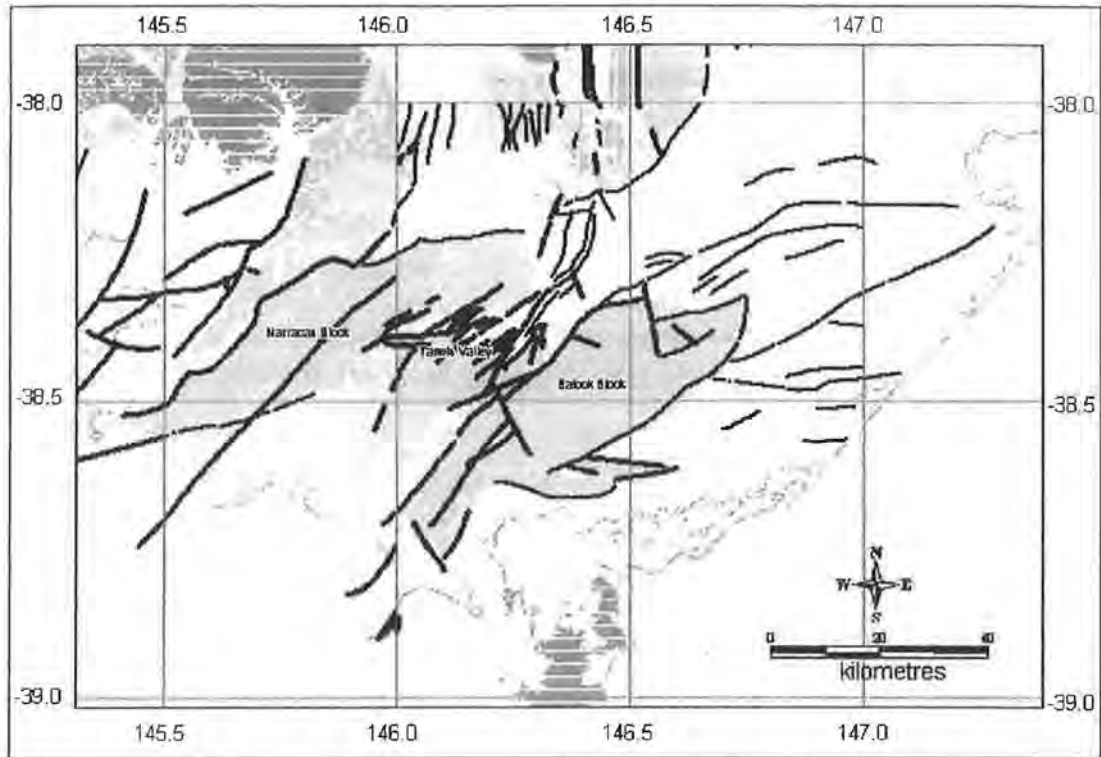


Figure 2: Geology of the Strzelecki Ranges, Gippsland

In 1964 the first seismograph was installed in Gippsland by the Australian National University. Currently there are five permanent seismographs, and two accelerographs in the Gippsland area. The Seismology Research Centre operates all of these instruments, three on behalf of Loy Yang and Hazelwood Power stations.

The catalogue of earthquakes in the Gippsland area includes 19 events of magnitude ML 4 or greater since 1900. The largest event recorded in Gippsland was of magnitude ML 5.6 located within the Strzelecki Ranges at Boolarra in 1969 (denoted by the light coloured circle in figure 1). The 1969 Boolarra earthquake was felt strongly throughout Gippsland and was also felt in Melbourne. During the earthquake, circuit breakers at Yallourn, Morwell East, Leongatha, and Ferntree Gully were tripped, causing power outages for up to 20 minutes (Wilkie, 1970).

3. STRZELECKI SEISMOGRAPH NETWORK

During August 2000 a relatively dense seismograph network was installed in the Strzelecki Ranges. The network consisted of seven seismographs, three on rock sites and four on soil sites (Figure 3). The soil sites were located on Cretaceous sands and gravels (SBSV, SGTH), deeply weathered Tertiary basalts (THOP), and Quaternary sands (SYRM).

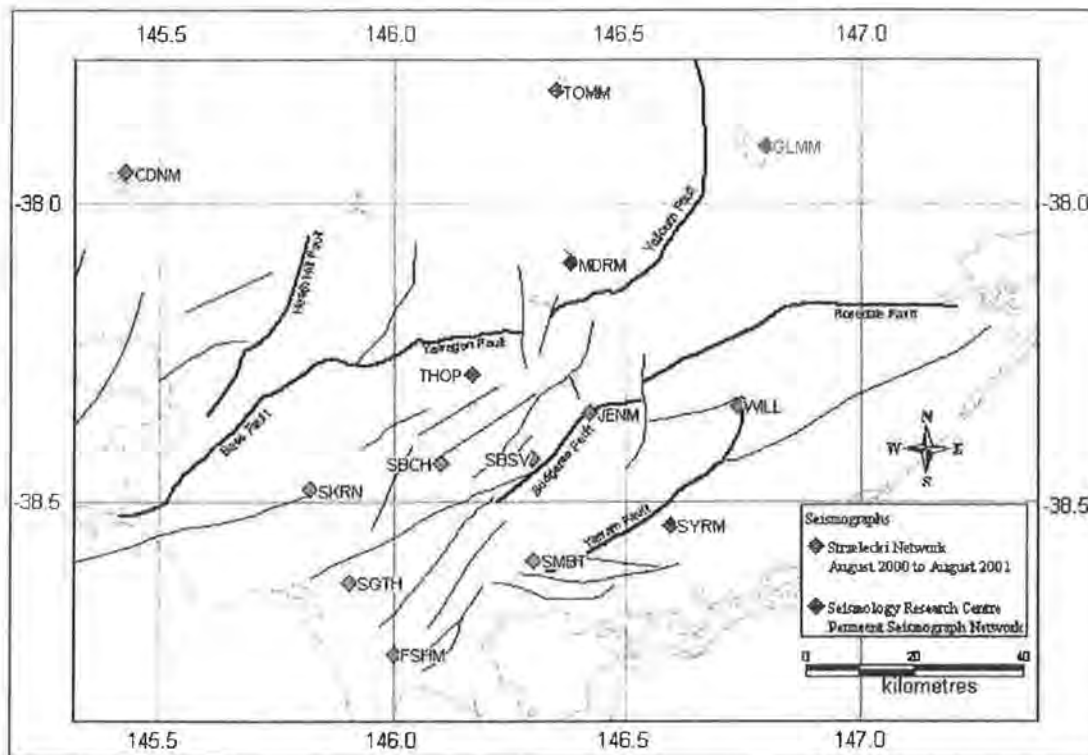


Figure 3: Strzelecki Seismograph Network

During the year that the Strzelecki network was operating, 31 earthquakes were located within the network. These earthquakes ranged in magnitude from ML 0.8 to 4.9. Depths range from 3 to 20 km. None of the earthquakes located in this study were as deep as some of the events located prior to 1979.

On 29 August 2000, just three days after the installation of the Strzelecki network, a magnitude ML 4.9 earthquake occurred near Boolarra South. This earthquake was the largest event to occur in the Gippsland region since 1969. Similar to the 1969 event, the 2000 earthquake was felt strongly in Gippsland and the Melbourne suburbs.

In late October 2000, a swarm of earthquakes began approximately 7 km to the southeast of Yarram (near SYRM in figure 3). This swarm was continuing in September 2001, with a total of 35 events recorded, when the SYRM seismograph was decommissioned. All of the events recorded had magnitude of ML 1 or less so were too small to be recorded on any of the other seismographs in the network. They occurred at various times during both the day and night, so were not blasts.

Figure 4 shows the location of the earthquakes that were located between August 2000 and September 2001. The spatial distribution of earthquakes is similar to that suggested by past seismic activity. The uncertainty in the easting and northing of the locations is less than 5 km. The depth uncertainty for the larger events, greater than magnitude 3, was also less than 5 km.

Focal mechanisms calculated for the three largest events suggest southeast to northwest compression and reverse faulting (Figure 5), which is consistent with other studies of stress in the region (Hillis, 2000).

A cross section through the Strzelecki Ranges perpendicular to the Yarragon and Yarram Faults shows the depth distribution of the earthquakes between August 2000 and September 2001 (Figure 6 and 7). There are too few accurately located earthquakes to delineate active faults. The data does suggest that there are shallow events occurring in the Tarwin Valley that can not be assigned to one of the larger bounding faults. They may be occurring on the smaller faults within the Tarwin Valley. Other events lie within the footwall blocks of the major faults.

The earthquakes located using the data from the Strzelecki Network had depths ranging from 3 to 20 km. The depths determined for some of the earthquakes located before 1979, had depths estimated as deep as 46 km. No earthquakes located during the 2000 – 2001 period were shallower than 3 km. This distribution of earthquake depths suggests that the seismogenic zone in Gippsland is about 20 km deep. This is shallower than the historic data would suggest.

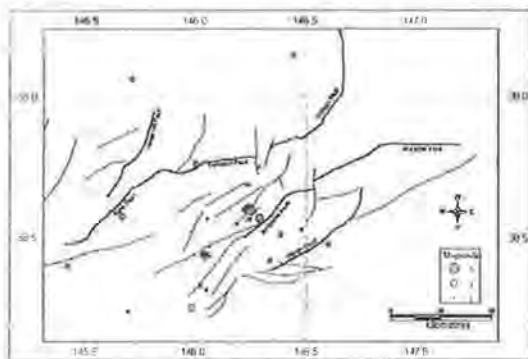


Figure 4: Earthquakes within the Strzelecki Ranges, August 2000 to September 2001



Figure 6: Plan View of Cross Section

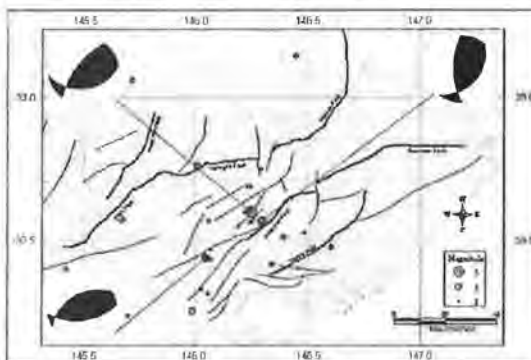


Figure 5: Focal Mechanisms of the three largest Strzelecki Ranges Earthquakes

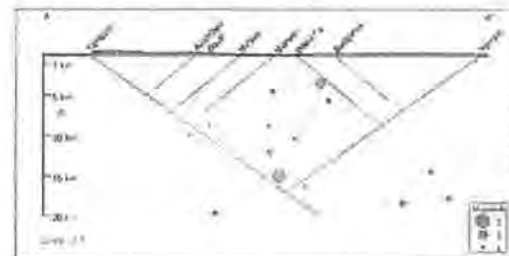


Figure 7: Cross Section – View looking northwest

4. IMPLICATIONS FOR EARTHQUAKE HAZARD IN GIPPSLAND

The good agreement of the fault and stress field orientation, the focal mechanisms and the depth distribution of the larger earthquakes (those located with uncertainties in depth of less than 5 km) suggest that the faults in the Strzelecki Ranges are active.

The absence of events in the top 3 kilometres may suggest that the seismic activity in the area is occurring in the Palaeozoic rock underneath the Cretaceous sediments on the Strzelecki Ranges.

5. CONCLUSIONS

Using the accurately located events from the Strzelecki seismograph network the depth distribution suggests that both the larger bounding faults and the smaller internal faults are active.

This study showed that the increase in accuracy in the locations gave a clearer picture of the spatial distribution of the events, particularly the depth.

Defining active faults using seismicity needs a large number of accurately located earthquakes. Using a relatively dense seismograph network, such as the one operated during this project, smaller events can be detected, thereby decreasing the minimum magnitude of completeness. Since there are many more small events than large, this significantly increases the rate of data accumulation. A dense network also helps reduce the uncertainty in larger events by increasing the number of arrival times available. More accurately located earthquakes with uncertainties of less than 5 km will reduce the time needed to gather a sufficient number of earthquakes to delineate active faults.

The data that has been collected is being used as a guide in refining seismotectonic models of Gippsland for earthquake hazard evaluation. The data will also be useful in studies into velocity models and attenuation.

6. ACKNOWLEDGMENTS

The research presented here would not have been possible without the support of the Australian Earthquake Engineering Society, who generously awarded Amy Brown a scholarship to run the Strzelecki Seismograph Network. The Seismology Research Centre provided in kind support by way of equipment and analysis software. Our thanks are also extended to Ian & Andrena Nunn, Kim Newby, Victor Love, Des Jennings, Robert Newton, Kath Harris and Neville Davis who allowed seismographs to be installed on their properties.

I would also like to thank Mike Jorgensen from URS for kindly sharing his research on identification of active faulting in Gippsland using geological information.

7. REFERENCES

- Douglas, J.G. (1988) Gippsland Basin. Geology of Victoria, edited by J.G. Douglas and J.A. Ferguson, p 228-234, Geological Society of Australia, Victorian Division, Melbourne.
- Hillis, R.R. and Reynolds, S.D., (2000) The Australian Stress Map. Journal of the Geological Society of London, Vol 157, p 915-921.
- Wilkie, J. R. (1970) The South Gippsland earthquake of 20 June 1969 BMR Record 1970/91, p 6.

IMPLEMENTATION OF ROUTINE PROCESSING TECHNIQUES FOR SOURCE PARAMETER DETERMINATION OF AUSTRALIAN EARTHQUAKES

TREVOR ALLEN
MONASH UNIVERSITY

AUTHOR:

Trevor Allen is a PhD student at the Department of Earth Sciences, Monash University, Melbourne. He is currently developing and improving methods to investigate source parameters of local and regional earthquakes

ABSTRACT:

Development of improved earthquake analysis software, which uses time and frequency domain analysis, forms the basis for this study. The software allows simple and rapid calculation of earthquake source parameters and conversion of digital time series recordings to true ground motion in terms of displacement, velocity and acceleration. Future development of the software will lead to the addition of focal mechanism solutions and other functions necessary to examine the earthquake source.

Seismic source parameters have been calculated for about 100 well located southeastern Australian earthquakes of magnitudes varying from M_L 1.2 up to M_L 5.1. Preliminary results illustrate a strong correlation between moment magnitude M_w (derived empirically from the seismic moment M_0) and local magnitude M_L , consistent with expected values. Static stress drop estimates ($\Delta\sigma$) tend to increase with increasing magnitude to at least M_L 5.1, contradicting the belief held by some authors that stress drop for natural earthquakes are self-similar over a large magnitude range.

1. BACKGROUND

In earthquake analysis in Australia and other regions, only hypocentral locations and local magnitudes M_L are routinely determined, with little attention being given to the determination of other source parameters such as seismic moment, stress drop and source dimensions. Advances in earthquake data acquisition and processing techniques, however, now allow for improved quantification of source parameters for local earthquakes.

The primary objective for this study is to provide improved software designed to make source parameter determination a routine procedure for local and regional earthquake analysis in Australia.

2. THEORY

Fourier analysis of an earthquake time series can reveal a great deal about the source and about the medium in which it occurs. Most seismic theories predict that the far-field displacement spectrum should remain constant at low frequencies, and become inversely proportional to some power of frequency at higher frequencies (Aki, 1967; Brune, 1970, 1971). Thus the far-field displacement spectrum can be described by three independent parameters: the low-frequency spectral level Ω_0 , the corner frequency f_c defined as the intersection of the low- and high-frequency asymptotes, and the slope controlling the decay rate of the high-frequency spectra (Figure 1).

Some source parameters that can be determined from spectral analysis include seismic moment, source dimensions and stress drop.

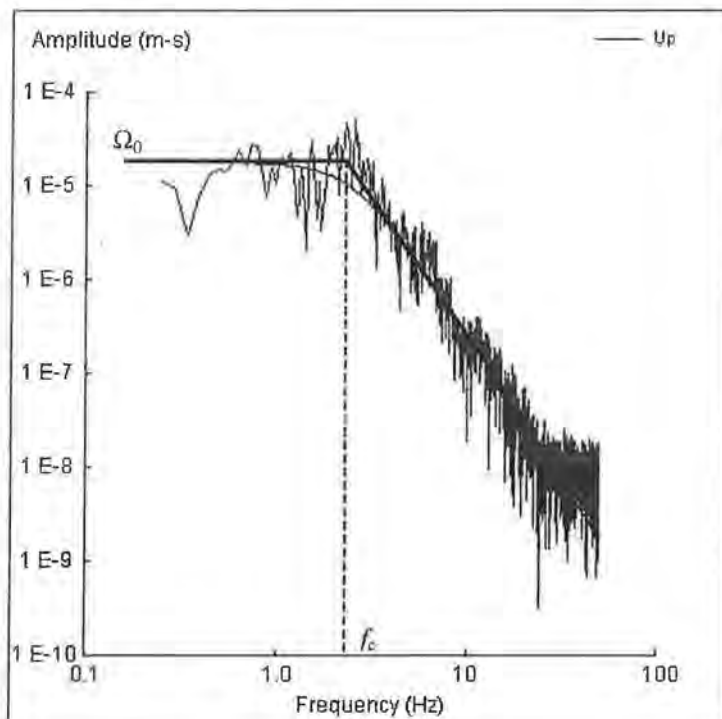


Figure 1. Example of S-wave far-field displacement spectra approximated by the low- and high-frequency asymptotes. The low-frequency spectral level Ω_0 is represented by the low-frequency asymptote while the corner frequency f_c is defined as the intersection of the two asymptotes.

2.1 Seismic Moment

The seismic moment M_0 is the most reliable measure of an earthquake's size. It is a physical measurement defined in terms of parameters of the double-couple shear dislocation source model. M_0 is expressed as follows (Aki and Richards, 1980)

$$M_0 = \mu \bar{u} A, \quad (1)$$

where μ is the shear modulus at the source, \bar{u} is the average displacement across the rupture, and A is the fault area. M_0 can occasionally be calculated using relation (1) whenever the average displacement across the fault is accessible for measurement. In practice, however, seismic moment is estimated from the spectral parameter Ω_0 from seismic waveform data in frequency domain (Figure 1).

The low-frequency spectral level Ω_0 of the far-field displacement spectrum is directly related to the seismic moment (e.g. Gibowicz and Kijko, 1994)

$$M_0 = \frac{4\pi\rho_0 c_0^3 R \Omega_0}{F_c R_c S_c}, \quad (2)$$

where ρ_0 is the density of the source medium, c_0 is either the P - or S -wave velocity at the source, R is the distance between the source and receiver, and F_c , R_c and S_c account for seismic wave radiation, free surface amplification and site correction for P - and S -waves respectively.

2.2 Moment Magnitude

Moment magnitude M_w can then be determined empirically from seismic moment employing the following definition by Hanks and Kanamori (1979)

$$M_w = \frac{2}{3} \log M_0 - 6.06, \quad (3)$$

where M_0 is in N·m.

2.3 Source Dimensions

Unlike the seismic moment calculation from relation (2), estimates of earthquake source dimensions are highly model dependant and are susceptible to systematic errors. The radius r_0 of a circular fault is inversely proportional to the corner frequency and is given by

$$r_0 = \frac{K_c \beta_0}{2\pi f_c}, \quad (4)$$

where K_c is a constant depending on the source model and β_0 is the S -wave velocity in the source area. The most commonly used model that of Brune (1970, 1971), represented by a circular dislocation with instantaneous stress release, where the constant $K_c = 2.34$.

2.4 Stress Drop

Of the different methods for estimating stress release, the static stress drop represents stress change during earthquakes the most accurately. Static stress drop is defined as the average difference between the initial and final stress levels over the fault plane. When complete stress release is assumed, the stress drop $\Delta\sigma$ from the relation is (Brune, 1970, 1971)

$$\Delta\sigma = \frac{7}{16} \frac{M_0}{r_0^3} \quad (5)$$

The relationship represents a uniform decrease in shear stress acting to produce seismic slip over a circular fault.

3. EQSOURCE

eqSource uses Fourier time series analysis for simple and rapid attenuation correction employing a frequency dependant quality factor $Q(f)$ (Wilkie and Gibson, 1994), and earthquake source parameter determination (e.g. seismic moment, moment magnitude, stress drop and source dimensions). One attribute of eqSource is that it is written in Java and is therefore cross-platform with good graphics capabilities. The software was written to provide a more user-friendly alternative to, and to extend routine source parameter determination beyond hypocentral locations and local magnitudes for Australia and other regions.

The software includes calibration of seismic recording apparatus to facilitate the simple conversion of digital time series recordings (measured in counts) to true ground motion in terms of displacement (mm), velocity (mm/s) and acceleration (mm/s²). In addition, eqSource also includes calculation of synthetic seismograms for a Wood-Anderson torsion seismograph on which Richter (1935) first defined the local magnitude M_L scale.

It is intended that in future developments, eqSource will include focal mechanism solutions and will also be able to read common waveform file formats (e.g. SeisMac, PC SUDS, Seisan and GSE). In addition, it is intended to introduce a genetic algorithm for automatic moment magnitude determination (Ottemöller and Havskov, 2001).

4. PRELIMINARY RESULTS

About 100 well located events were selected to investigate source parameters for earthquakes in southeastern Australia. The magnitude of the events ranged from M_L 1.2 to M_L 5.1.

A comparison between M_L and M_W was performed to test the precision of eqSource's magnitude determination functions. The test illustrated a strong correlation between the two magnitude scales. Magnitudes for both M_L and M_W tend to be equal around magnitude 2.5, while for local magnitude M_L 5.0, moment magnitude M_W was observed to be about 4.5. These results are consistent with the findings of Wilkie (1996).

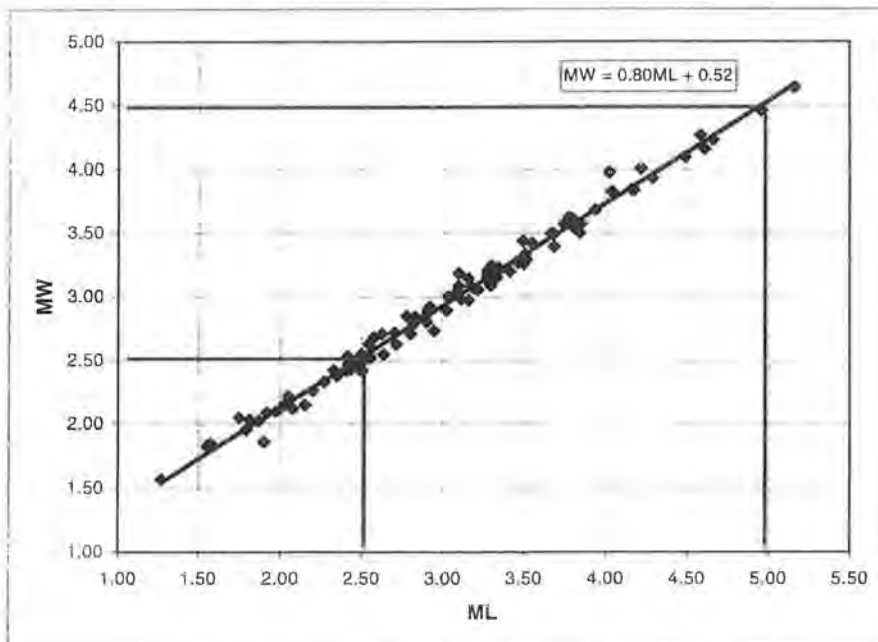


Figure 2. Plot of M_W vs. M_L for the selected events determined employing eqSource for selected southeast Australian earthquakes.

Average static stress drops for intraplate earthquakes have been reported to range from 0.1 to about 100 MPa (Johnston, 1992; Abercrombie and Leary, 1993) although most do not exceed 10 MPa. Many studies show an apparent breakdown of self-similarity (the notion of constant stress drop for all earthquake magnitudes) at low magnitudes (Shi, *et al*, 1998; and others) however, it has been argued that seismic attenuation for small earthquakes may obscure the measurement of corner frequencies, which facilitates the calculation of $\Delta\sigma$ (Abercrombie and Leary, 1993; and others). Stress drop determinations from southeastern Australian earthquakes, however, tend to increase with magnitude up to at least M_L 5.1 to unusually high values of about 50 MPa (Figure 3). This behaviour is indicative of a highly stressed medium and has been observed in other stable continental regions (Johnston, 1992; Burton, 2001).

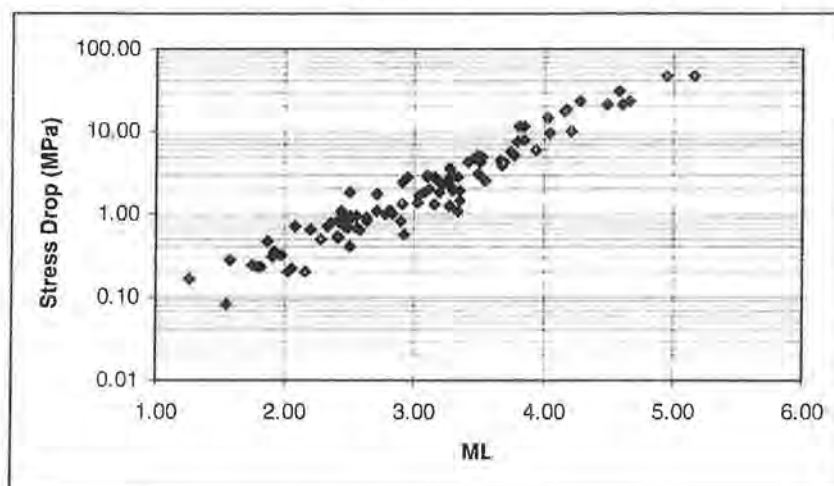


Figure 3. Stress drop vs. local magnitude M_L for selected southeast Australian earthquakes.

Given that the rupture radius is inversely proportional to the cube root of stress drop and values for stress drop are high, we also find that earthquake rupture size, for any given magnitude, tend to be smaller than normal.

5. SUMMARY

The development of improved source parameter calculation software has provided a more user-friendly alternative for routine source parameter determination of earthquakes. Implementation of the software will further extend our understanding of the *in-situ* stress conditions of the Australian continental landmass and will assist in more reliable, future earthquake hazard estimates.

Preliminary data acquired employing eqSource has shown that the stress drops of southeast Australian earthquakes do not appear to be self-similar and tend to increase with magnitude up to at least M_L 5.1, implying that the southeast Australian region is under a high degree of stress. This can be validated from previous *in-situ* rock stress measurements (Denham, et al, 1979; and others).

6. REFERENCES

- Abercrombie, R. and Leary, P. (1993) Source parameters of small earthquakes recorded at 2.5 km depth, Cajon Pass, Southern California: Implications for earthquake scaling. *Geophys. Res. Lett.*, Vol 20, pp 1511-1514.
- Aki, K. (1967) Scaling law of seismic spectrum. *J. Geophys. Res.*, Vol 72, pp 1217-1231.
- Aki, K. and Richards, P. G. (1980) *Quantitative seismology; theory and methods: Volume 1.* W. H. Freeman and Company, San Francisco, pp 557.
- Brune, J. N. (1970) Tectonic stress and the spectra of seismic shear waves from earthquakes. *J. Geophys. Res.* Vol 75, pp 4997-5009.
- Brune, J. N. (1971) Correction to tectonic stress and the spectra of seismic shear waves from earthquakes. *J. Geophys. Res.* Vol 76, pp 5002.
- Burton, P. (2001). Pers. comm.
- Denham, D., Alexander, L. G. and Worotnicki, G. (1979) Stresses in the Australian crust: evidence from earthquakes and *in-situ* rock stress measurements. *BMR J. Aust. Geol. Geophys.* Vol 4, pp 289-295.
- Hanks, T. C. and Kanamori, H. (1979) A moment-magnitude scale. *J. Geophys. Res.*, Vol 84, pp 2348-2350.
- Gibowicz, S. J. and Kijko, A. (1994) *An introduction to mining seismology.* Academic Press, New York, pp 339.
- Johnston, A. C. (1992) Brune stress drops of stable continental earthquakes; are they higher than "normal" and do they increase with seismic moment? *Seism. Res. Lett.*, Vol 63, pp 609.
- Ottmøller L. and Havskov, J. (2001) Robust and fast automatic moment magnitude determination using a genetic algorithm. Submitted to; *Bull. Seism. Soc. Am.*
- Richter, C. F. (1935) An instrumental earthquake magnitude scale. *Bull. Seism. Soc. Am.*, Vol 25, pp 1-32.
- Shi, J., Kim, W.-Y. and Richards, P. G. (1998) The corner frequencies and stress drops of intraplate earthquakes in the northeastern United States. *Bull. Seism. Soc. Am.*, Vol 88, pp 531-542.
- Wilkie, J. R. (1996) Earthquake source parameters, Victoria, Australia. Ph.D. Thesis, La Trobe University, Melbourne, pp 218.
- Wilkie, J. and Gibson, G., (1994) Estimation of seismic quality factor Q for Victoria, Australia. *AGSO J. Aust. Geol. Geophys.*, Vol 15, pp 511-517.

CADOUX SWARM SEPTEMBER 2000 – AN INDICATION OF RAPID STRESS TRANSFER ?

MARK LEONARD
AGSO GEOSCIENCE AUSTRALIA

AUTHOR:

Mark Leonard - In 1996 obtained a PhD from the Research School of Earth Sciences of the Australian National University, in seismology. Thesis: Noise characterisation and secondary phase detection using multicomponent seismic data. In 1986 obtained a B.Sc.(Hons.) from the University of Adelaide, in geophysics.

Has worked for AGSO - Geoscience Australia since 1990, in a number of roles including: Nuclear Monitoring, Seismic Network Operations, Software Engineering, Earthquake Monitoring and Neotectonics. In 1987 to 1989 worked for several land seismic companies in central Australia.

Research interests include: the seismicity of Australia, correlating seismicity to geology, earthquake location, signal processing, onset time pickers, S phase detectors, microseismic noise, neotectonics of the Australian crust and developing a seismicity model of Australia.

Cadoux Swarm September 2000 - an indication of rapid stress transfer?

M. Leonard & P. Boldra AGSO - Geoscience Australia, GPO Box 378, Canberra ACT 2600, Australia

Introduction

An earthquake swarm occurred about 25km north of Cadoux during September and October 2000. The swarm consisted of 1700 recorded earthquakes, the largest of which was magnitude 3.6. As many of the locals remember the 1979 6.7 Cadoux earthquake, the swarm was of considerable interest to the local community. Seismologically swarms are a poorly understood phenomena and despite being relatively common in Australia have not been well studied. Swarms occur, on average, every 1-2 years in SW Western Australia and every 3-6 years in eastern Australia (Pers. Com. Gary Gibson). This paper analyses this swarm and notes some of the implications of this swarm for stress transfer in SW Western Australia.

The Earthquakes

Between September 10 (day 254) and October 8 (day 282) the seismic station BLDU, located 35-40km east of the location of the swarm, recorded 1700 earthquakes. On September 21 four temporary stations were deployed. Whilst these proved to be much less sensitive than the permanent stations, earthquakes that they did record were very well located as we had up to 3 stations with good azimuthal coverage within 20 km of the events. Unfortunately there was a problem with the stations which was located within 3 km of the bulk of the events and from which we obtained only about 10 events. Of the 1700 earthquakes we have magnitudes for 500, locations for 120 and accurate locations for 80. All the earthquakes are thought to be about 2km deep, with Rg being observed for several events and the well located events all having depth less than 5km.

An event is considered well located if the EW error + NS error is less than 30 km. Figure 1 shows the location of the 80 well located earthquakes and their associated error ellipses, several of which are large. Figure 2 shows that the seismicity lies in four clusters on a NS trend, with the majority of the earthquakes in clusters C. The error ellipses of these 80 earthquakes are sufficiently small to be confident that these four clusters are real. Within the 95% error ellipses, it is possible to plot all the earthquakes onto just 4 points one for each cluster. Initial attempts to refine these locations using Joint Hypocentre Determination (JHD) methods failed to decrease the scatter of locations. This is due to inappropriate earth models and failure of the assumption that the azimuth from station to event is constant. Further work with more appropriate earth models and analysing the clusters separately will be performed in the near future.

Figure 3 shows a range of properties and features of the swarm. Magnitudes using BLDU data were calculated for 500 events, 114 of which also had KLBR magnitudes. The other southern WA stations were also used calculate magnitudes where possible. All the magnitudes were compared to ensure they were consistent and to confirm that BLDU shows no particular bias. There is a random error in any single station ML estimate and for this swarm I estimate the error is ± 0.4 ML. The 500 events are plotted in figure 3 and shows the swarm starting with two earthquakes on day 254 and two on day 259. Two ML 2+ events occur on day 260 followed by 200 events on that day including 1 ML 3+ event. The activity then gradually lessens with other peaks in activity on days 263/264, 269 and 283.

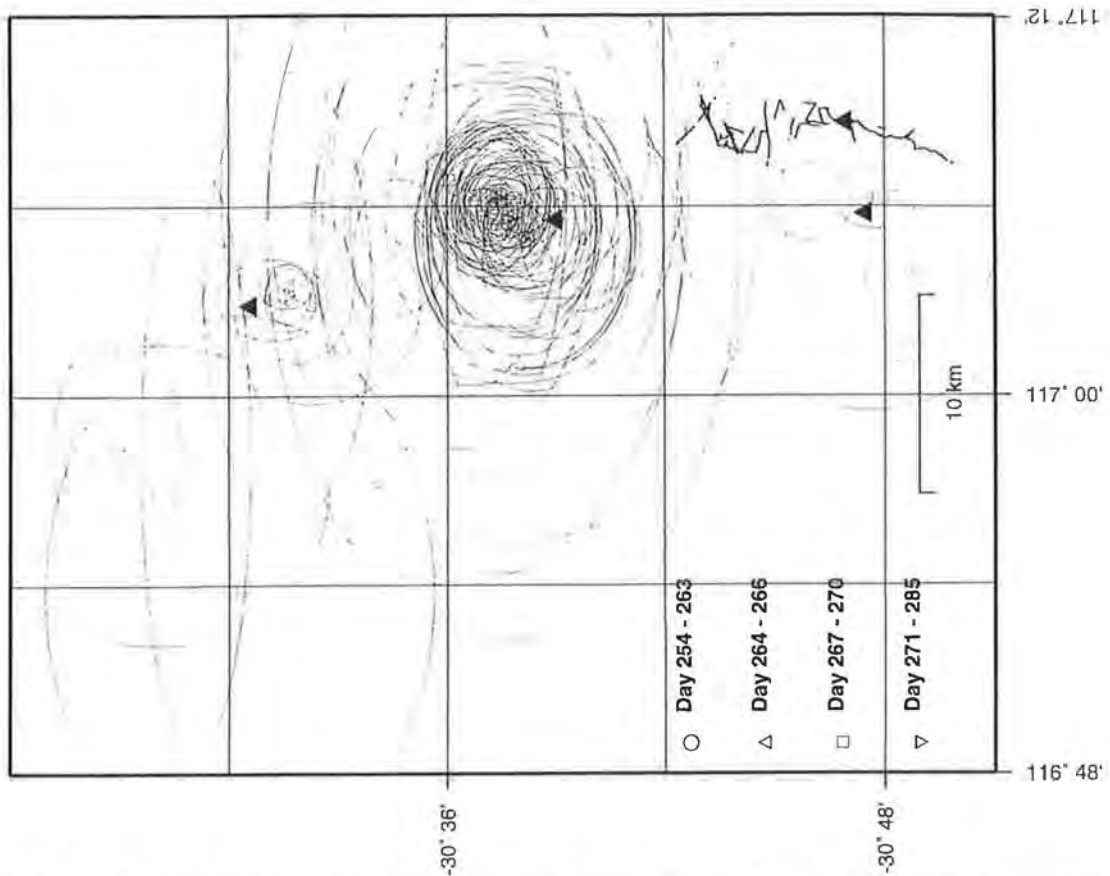


Figure 1: The 79 well located events with their 95% error ellipses plotted, the closest 3 seismographs and the fault trace of the 1979 earthquake.

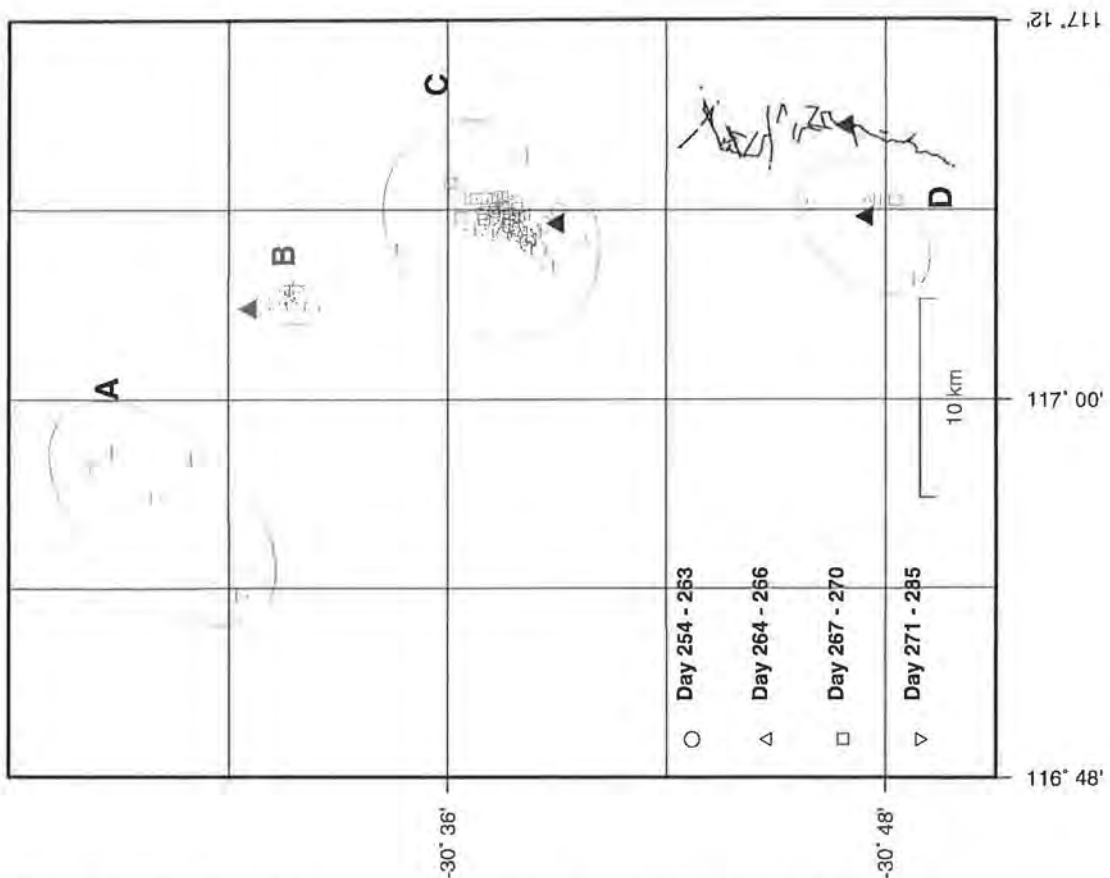


Figure 2: The 79 well located events and the four clusters within which they are located.

	A	B	C	D	Total
254-263	0	1	19	0	20
264-266	0	1	17	2	20
267-270	0	0	19	1	20
271-285	5	5	7	2	19
Total	5	7	62	5	79

Table 1: Summary of the number of well located events in each cluster for different times during the swarm.

The next plot in figure 3 shows the number of earthquakes per day, the cumulative number of the 1700 earthquakes observed on BLDU and the cumulative number of the 500 earthquakes for which magnitudes could be calculated. These all reflect the activity level discussed above. The similar shape of the two cumulative plots suggests that the 500 events are a consistent 30% of the total number of events per day. ab plots indicate that the b value during the swarm remained constant and that the data is complete down to magnitude 0.6, below which the data is very incomplete. This suggests that almost all the extra 1100 events have magnitudes less than ML 0.6.

The next plot in figure 3 shows the cumulative energy release during the swarm and cumulative area of fault ruptured by the swarm. They were calculated from the 500 events for which a magnitude was determined. The 6 largest earthquakes account for more than 50% of the energy released by the 500 events and, given the very small size of the other 1100 events, probably 50% of the total energy released by the swarm. This confirms that for this swarm, the well known phenomena of the bulk of the energy released by earthquakes is released by the largest handful of events. The largest events also account for most of the rupture area but not to the same extent as they do for the energy. A magnitude 3 earthquake has an area of 0.1 km² with a displacement of 16 mm and a magnitude 2 has an area of 0.005 km² and a displacement of 3 mm. I estimate that the area of the other 1100 events is approximately counter balanced by many of the smaller events re-rupturing areas of the fault. Given these uncertainties and the uncertainty of the formula for calculating the area of a fault, the area could easily vary by 50%.

Rapid stress transfer

Figure 2 shows the data clustered into 4 areas. The location errors are sufficiently large that, within their 95% error ellipses, all the earthquakes can be relocated to just four points, one for each of the clusters. Whilst we can't prove that this is the case, the clusters are real and within their 95% error ellipse the earthquakes cannot be relocated to one point. The 79 earthquakes have been plotted using different symbols based on when during the swarm they occurred. It is clear from figure 2 that the four clusters have a temporal pattern, with earthquakes in cluster A only occurring in the last 20 earthquakes. Table 1 summarises the distribution of earthquakes with time. Clusters A and B are much more active in the last phase of the swarm and cluster C is relatively quiet in the last phase.

This temporal and spatial distribution of earthquakes suggests that there has been a stress transfer from around clusters C during the first 16 days (10 days if the two events on September 10 are ignored) of the swarm, to cluster A during the last 14 days. The total area of faults in this swarm was about 1.5 km² with an average displacement of about 10mm. The transfer of sufficient stress the 20 km between cluster C and A to trigger earthquakes in cluster A is surprising. Further investigations of stress transfer is

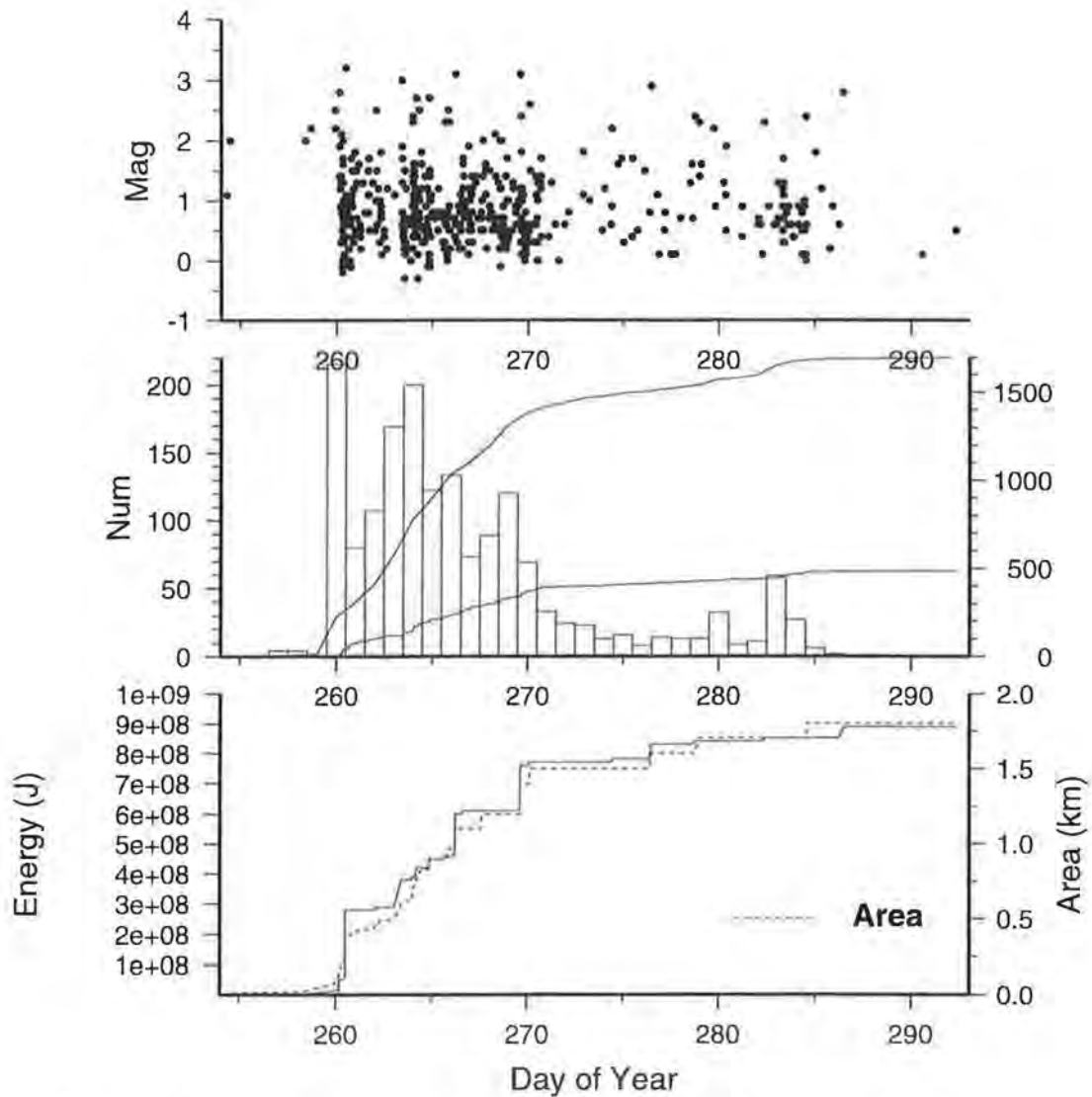


Figure 3: Some features of the earthquake swarm. In plot 1 each of the 500 earthquakes for which magnitudes were calculated are plotted. Plot 2 is the number of earthquakes per day recorded on BLDU, with the scale on the left. The two curves are the cumulative number of earthquakes recorded on BLDU and the cumulative number for which magnitudes were calculated. Plot 3 is the cumulative energy released and cumulative area ruptured by the swarm.

required but this result does raise questions of; how much stress can be transferred by small earthquakes, how fast this stress can be transferred distances of tens of kilometers and how close to failure this area of the Australian crust might be?

RECURRENCE RELATIONSHIPS FOR AUSTRALIAN EARTHQUAKES

CVETAN SINADINOVSKI⁽¹⁾ AND KEVIN MCCUE⁽²⁾
AGSO GEOSCIENCE AUSTRALIA⁽¹⁾ AND ASC⁽²⁾

AUTHORS:

Cvetan Sinadinovski has an Honours and a M.Sc degree in Geophysics from the School of "A.Mohorovicic" at Zagreb University, and a PhD in the field of geotomography from the Flinders University in South Australia. He has worked as a visiting fellow in USA and Europe, and as a software specialist in Sydney and Adelaide. Currently employed as a professional officer in the Urban Geoscience Division of AGSO Geoscience Australia in Canberra. Member of the Australian Institute of Geoscientists, Association of Physicists of Macedonia, and AEES.

Kevin McCue is an engineering seismologist at ASC with a strong interest in the Neotectonic history of Australia. He has worked in a range of seismo-tectonic environments in Europe, Antarctica, Papua New Guinea and Australia and investigated recent faults in Mongolia and Turkey. He is a Fellow of IEAust and scribe of three of the Standards working groups for the latest revision of the Loading Code.

ABSTRACT:

The relationship between the number of earthquakes and their magnitude in any time interval is routinely approximated by a Gutenberg and Richter formula which leads to a straight line in log-linear coordinates. Worldwide data are often better fitted by a bi-linear curve over the recorded magnitude range and the discontinuity point can be explained in physical terms.

The bi-linear pattern emerges on both large scale such as the whole of Australia and small (zone) scale, such as southeast Australia. In that case usage of the straight-line fit will overestimate the occurrence rate of large events and underestimate the rate in the mid-magnitude range. This is an important consideration when estimates of maximum magnitude are required for periods much longer than the observation time, especially in zones where few large earthquakes have been recorded

1. INTRODUCTION

The seismicity of the Australian continent is typical of that experienced for intra-plate environments. Australian earthquakes are shallow and most of the focal mechanisms are consistent with horizontal compression. The earthquakes in continental interiors are associated with high local stress concentration and relatively short fault rupture lengths. In the last hundred years, 26 earthquakes with a magnitude of 6.0 or greater were recorded in Australia, and on average there were two to three earthquakes per year with a magnitude of 5.0 or more (AGSO Earthquake Database).

The frequency distribution of earthquakes as a function of their magnitude is of primary importance for seismic investigations. Hazard outputs depend on the definition of the seismogenic areas or zones. In situation where faults and other tectonic structures are not obvious at the surface the shape of the seismic zones can not be clearly defined. If some region is too small for the period of monitoring then the apparent frequency of large events can only be obtained by extrapolation of the frequency of observed small events, but the uncertainty in the estimated frequency is very high. Instead, a larger area can be taken to compensate for the short time interval provided the tectonics and underlying geological processes are similar. Zones can be chosen according to the criteria of earthquake clustering in the continental crust. The pattern of earthquakes with magnitude $M \geq 4.0$ is sufficient for zoning in Australia (Fig.1).

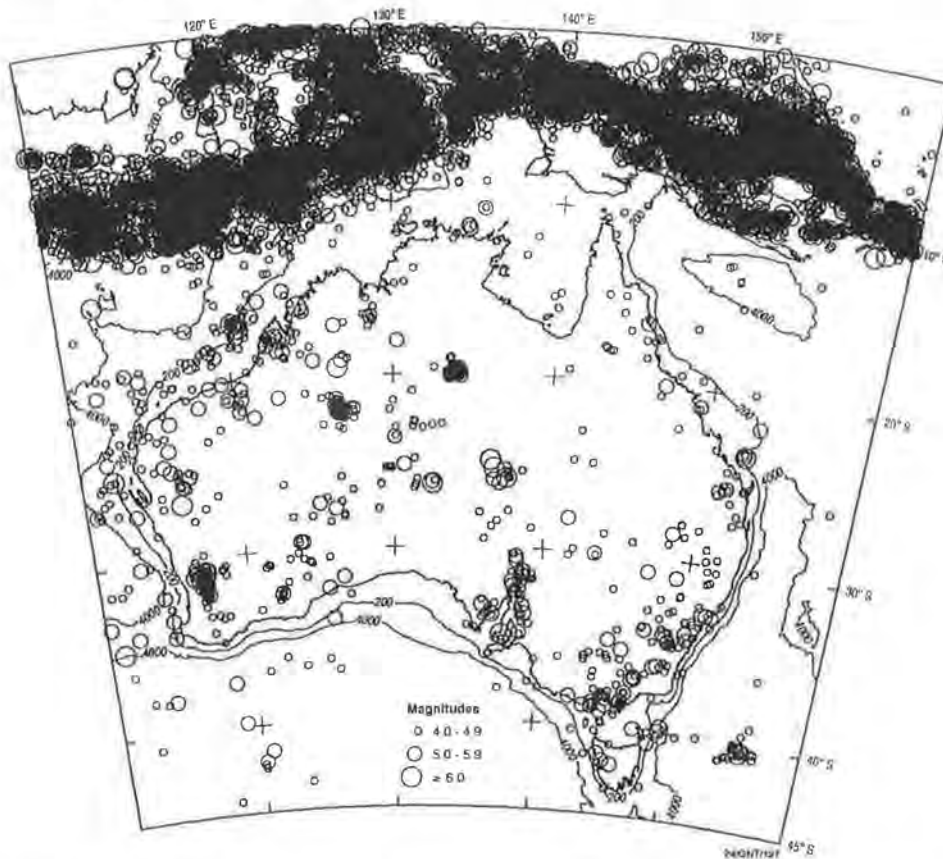


Fig.1. Epicentral map of all earthquakes in the last 100 years with magnitude $M \geq 4.0$

One recent model (McCue et al., 1998), defines the zones according to the pattern of shear failure under north-south compression of the continent. Statistics also show that Western, Central and Eastern Australia are different and these areas can be considered to be separate zones for assessing earthquake recurrence times (Sinadinovski, 2000).

2. DATA

The data used for this study comprise a subset of the AGSO earthquake database for Australia between 10 and 45°S and 110 and 155°E. Analysis was restricted to only those time intervals in which the seismic network was able to consistently record all earthquakes of the specified magnitude in the Australian continent. On our assessment, the periods of completeness were 1901-1999 for $M \geq 6.0$, 1959-1999 for $M \geq 5.0$, 1965-1999 for $M \geq 4.0$, and 1980-1999 for $M \geq 3.2$.

Numbers of earthquakes were counted for the declustered dataset of magnitude 3 and more in magnitude intervals of 0.2 which is about the uncertainty in magnitude. The dataset referred to as a declustered data set, has the same magnitude ranges but the identifiable foreshocks or aftershocks have been removed. A quake was considered to be a foreshock or an aftershock and was removed if:

- it was within a certain distance d km of the main shock (McCue, 1990) where

$$d = 10^{(M-4.11)/1.65} \quad \dots(1)$$

and M is the magnitude of the main shock and

- if the quake occurred within 10 years for magnitude 7, within 1 year for magnitude 6, within 3 months for magnitude 5, and within 10 days for magnitude 4 (McFadden *et al.*, 2000).

3. METHODOLOGY

The relation between the number of earthquakes and their magnitude is routinely approximated by the Gutenberg and Richter empirical formula (Gutenberg and Richter, 1949) represented by a single straight line in log-linear coordinates

$$\log N = a - bM \quad \dots(2)$$

where N is the cumulative number of earthquakes per year, M is the local or Richter magnitude and a , b are constants related to the level and the slope. Data are treated by grouping of N according to the magnitude range.

The coefficient b usually takes a value around 1. In general this relationship fits the data well on a global scale, but not for particular tectonic regions. Various authors have discussed the spatial variation in b . For example, Kárník (1971) mentioned that in some cases for the weakest and the strongest earthquakes, the $(\log N, M)$ distribution deviated significantly from linearity. Recently, some other approximation formulae have been applied (Utsu, 1999, and Kagan, 1999).

For use in prediction and comparative mechanism studies, standard errors of b must be supplied for statistical tests. Because earthquakes are stochastic processes and the b value is a random variable, knowledge of the probability distribution and the variance of b are essential in studying its temporal and spatial variation. The b value can be calculated by least-squares regression, but the presence of even a few large earthquakes influences the resulting b value significantly. Alternatively, the maximum likelihood method can be used to estimate b because it yields a more robust value when the number of infrequent large earthquakes changes.

There are cases, however, where the least-squares method is more suitable. The distribution of the best estimate can then be tested against a standard χ^2_n , a chi-squared distribution for n degrees of freedom, where n is the number of events above certain magnitude threshold.

4. ANALYSIS

Data extracted from the AGSO earthquake database were declustered within the described parameters. The magnitude ranged from ML3.2 to ML7.2. Figure 2 is a plot of the cumulative number of counted earthquakes per year in Australia against magnitude.

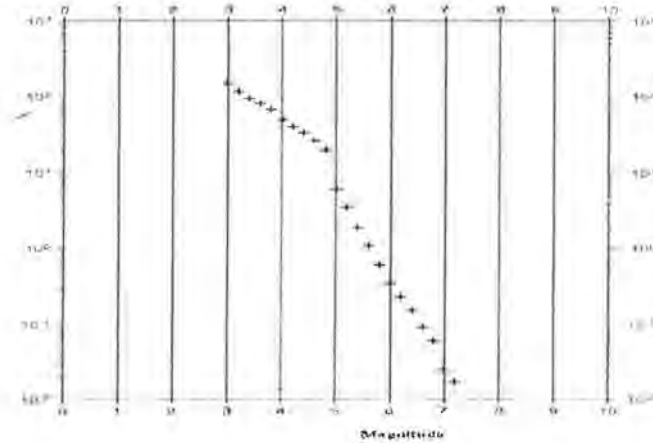


Fig. 2. Plot of the cumulative number of earthquakes per year in Australia against the magnitude (declustered data)

From the diagram it is obvious that a straight line is not a good fit, particularly for the larger earthquakes, and approximation with two linear segments is more representative. There is a significant change of slope around magnitude 5.2 ± 0.1 and that position was also noticed for the three zones identified as Western, Central and Southeastern Australia (Sinadinovski, 2000).

The Southeastern Australia zone was defined as rectangle extending from northern Bass Strait into Queensland (Fig. 3-a). The coefficients for its straight line least-squares-fit (solid line on Fig. 3-b) were calculated as $a = 4.3$ and $b = 0.98$.

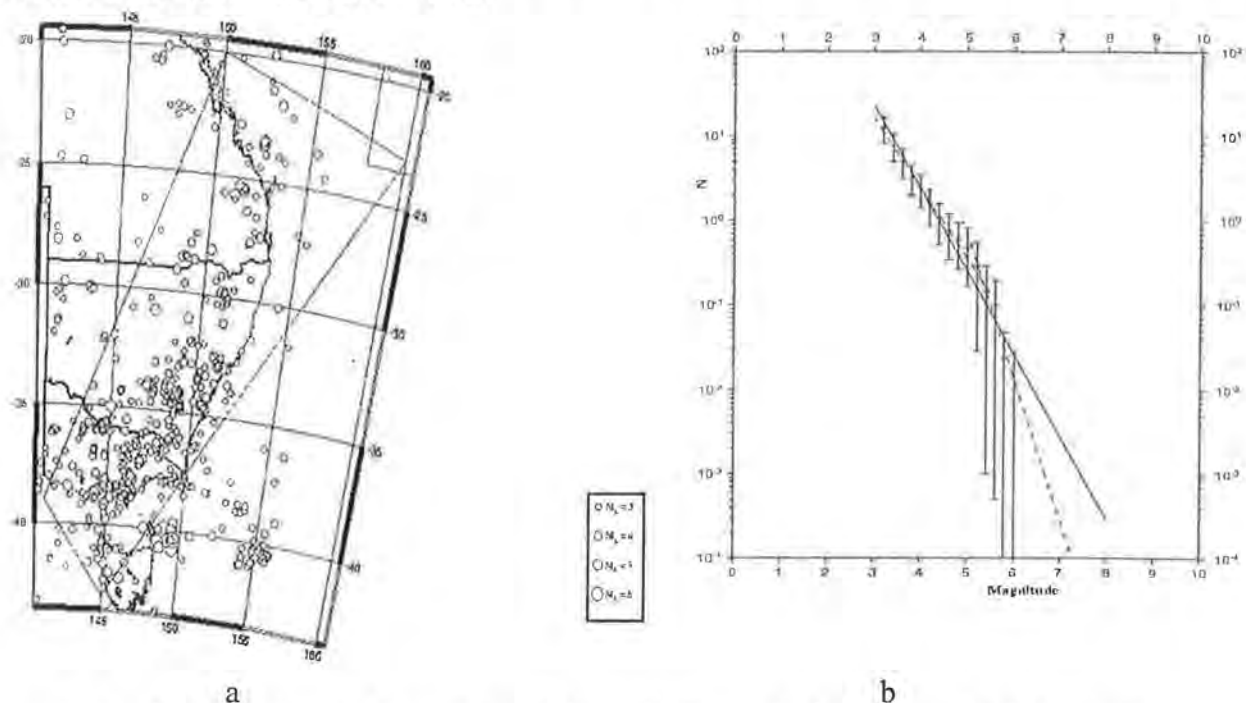


Figure 3: Southeastern Australia zone, seismicity and its magnitude-frequency relationship

5. RESULTS AND DISCUSSION

From the graph it is evident that a straight line does not fit well and earthquakes above magnitude 5 have much larger error bars because they are so few. Therefore an approximation with two linear segments represented by dashed lines is much more suitable. For the upper segment with magnitudes between 3.2 to 5.1 the calculated b value was 0.83 ± 0.09 , while for the lower segment with magnitudes $M \geq 5.2$, the calculated b value was 1.7 ± 0.48 .

Again there is a significant change of slope around magnitude 5.2, which is consistent with our previous observations. Kárník (1971) related the discontinuity point to the fracturing of the material subjected to stress, while Aki (1999) explained the discontinuity through physical terms of source size saturation effects. It is accepted that most earthquakes in stable continental regions only occur in the brittle upper crust and that above a certain magnitude at which the whole width of the brittle crust is ruptured the magnitude can only increase by rupturing a longer fault zone at constant width. That situation should occur at a magnitude around 6 where one could expect another cusp.

A chi-squared χ^2_n -test was performed to assess which of the linear and bi-linear recurrence relations best matched the observed distribution of events in the Southeastern Australia zone with magnitudes greater than 5. The test results show that the probability of the observed distribution being produced by the bilinear fit is much higher than with the straight line, namely 98% as opposed to only 18%.

We have revised the b values for Southeastern Australia using new information which became available following a recent AGSO marine geophysics cruise off the coast of Tasmania. A large sequence of felt earthquakes off Flinders island in the 1880's and 1890's and a later event in the 1940's were excluded from our original analysis because they were thought to be associated with a hypothesised hotspot under northern Tasmania. The marine cruise found no evidence that a hotspot exists there, no submarine volcanoes or major faulting on the continental shelf.

We concluded that the earlier observed seismicity should be included in a slightly modified source zone in Southeastern Australia. Including the declustered events, the largest of the sequence and the 1946 event resulted in a remarkable reduction in both the b value and its apparent uncertainty. The revised analysis produced a b value of 1.14 ± 0.08 , the upper limit of the range, 1.22 overlaps with the lower limit of range of the previous findings.

Because the value of b is observed to change with time and space, its mean and variance might also be expected to change. In other words, b should be regarded, in general, as a non-stationary stochastic process. When sampling with a small time and space window, however, b can usually be taken as stationary and with constant consideration of its characteristics.

On the basis of these results it can be concluded that the straight-line fit overestimates the frequency of large events and underestimates the frequency of moderate size events and the bi-linear model better fits the recurrence of Australian earthquakes. This is especially critical when estimates of maximum magnitude are required for periods much longer than the observation time in zones where only a few large earthquakes have occurred. For example, the values of maximum magnitude defined in Southeastern Australia as the 10,000-year magnitude are 7.1 and 8.4 respectively. The effects on the 500-year pga as used for the Australian Building Code AS1170.4 are minor. This study shows that the same pattern emerges on both large (whole country) and small (zone) scale. However, the statistics are only a quantitative indication as it is not possible to estimate in detail the crustal stress in a region, nor to determine its exact physical status.

6. REFERENCES

- Aki, K. (1999) Scale dependence in earthquake processes and seismogenic structures, ACES Workshop, Brisbane, pp 437-441.
- Gutenberg, B. and Richter, C.F. (1949) Seismicity of the Earth and associated phenomena, Princeton Univ. press.
- Kagan, Y.Y. (1999) Universality of the Seismic Moment-frequency Relation, Pure and Applied Geophysics, 155, pp 537-573.
- Kárník, V. (1971) Seismicity of European Area - Part 2, D. Reidel Publishing Company, Dordrecht, Holland.
- McCue, K.F. (1990) Australia's large earthquakes and recent fault scarps, J. Structural Geology, Vol 12, No 5/6, pp 761-766.
- McCue, K.F., Somerville, M., and Sinadinovski, C. (1998) GSHAP and the proposed Australian earthquake hazard map, AEES conference, Perth, pp 18/1-5.
- McFadden, P., Sinadinovski, C., McCue, K.F., and Collins, C. (2000) Is earthquake hazard uniform across Australia?, AGSO report, Canberra.
- Sinadinovski, C. (2000) Computation of recurrence relation for Australian earthquakes, AEES conference, Hobart, pp 22/1-5.
- Utsu, T. (1999) Representation and Analysis of the Earthquake Size Distribution: A Historical Review and Some New Approaches, Pure and Applied Geophysics, 155, pp 509-535.

CLASSIFYING THE SEISMIC REGIONS OF AUSTRALIA

NICHOLAS WILLIAMS AND MARK LEONARD
AGSO GEOSCIENCE AUSTRALIA

AUTHORS:

Nick Williams - B.Sc. Monash University 1999, B.Sc (Hons) University of Tasmania 2000.

Affiliation: AGSO - Geoscience Australia, GPO Box 378 Canberra, ACT 2601.

Resume: Have worked at AGSO - Geoscience Australia since 2/2001, initially in the Urban Geohazards Division (Neotectonics Project), and subsequently in the Minerals Division. Research interests include ore deposit geology (especially alteration, geochemistry, and isotopic signatures), as well as earthquake hazard analysis.

Mark Leonard - In 1996 obtained a PhD from the Research School of Earth Sciences of the Australian National University, in seismology. Thesis: Noise characterisation and secondary phase detection using multicomponent seismic data. In 1986 obtained a B.Sc.(Hons.) from the University of Adelaide, in geophysics.

Has worked for AGSO - Geoscience Australia since 1990, in a number of roles including: Nuclear Monitoring, Seismic Network Operations, Software Engineering, Earthquake Monitoring and Neotectonics. In 1987 to 1989 worked for several land seismic companies in central Australia.

Research interests include: the seismicity of Australia, correlating seismicity to geology, earthquake location, signal processing, onset time pickers, S phase detectors, microseismic noise, neotectonics of the Australian crust and developing a seismicity model of Australia.

Classifying the Seismic Regions of Australia

Nicholas C. Williams and Mark Leonard

AGSO – Geoscience Australia, GPO Box 378, Canberra, ACT, 2601, Australia

Gutenberg-Richter Analysis of Australian Seismicity

Introduction

Gutenberg and Richter (1944, 1949) introduced the famous equation for the exponential distribution of earthquake magnitude:

$$\text{Log}_{10}(N) = a - bM$$

where N is the number earthquakes of magnitude M , and a and b are constants and the b value is considered to be an important parameter characterising seismicity in a region (Utsu, 1999). Different forms of this equation are used in the literature; the method used here defines N as the number of events of magnitude M or greater (after Gaull et al., 1990), and gives smoother curves when data is sparse (as in many regions of Australia).

A basic mathematical definition based on the formula indicates that higher a values are related to a higher level of seismicity, whereas higher b values are related to higher proportions of small events to large events. Researchers suggest that the b value varies spatially and temporally (see Utsu, 1999 for a list of relevant papers). It is important to note that a and b values can be affected by the magnitude scale and ranges used, and data completeness, so comparisons between regions should be done with care (Utsu, 1999).

Gaull et al. (1990) described 31 ‘source’ zones for earthquakes in and around Australia. These source zones were chosen based on geological, tectonic and geophysical data. They calculated b values for each zone for data up to 1984, using the maximum likelihood estimate method (MLE; Aki, 1965):

$$b = \frac{\log_{10} e}{M_{\text{avg}} - M_{\text{min}}}$$

where M_{avg} is the average magnitude of the sample, and M_{min} is the minimum magnitude for which the sample is complete. An alternative method is to use a normal least-squares method (LSM). Weichert (1980) discussed the advantages and disadvantages of each method; LSM places more weight on larger events (which are rare) whereas MLE places more weight on smaller events (which may not be completely recorded).

To aid the characterisation of Australian seismicity, a broad, first-pass analysis of Gutenberg-Richter values across Australia was carried out using these methods. The primary goals of this analysis were to help define zones in which data quality is good enough for further analysis, and to determine the broad characteristics for large regions of Australia, which can be later subdivided and characterised in depth.

Methods

Programs were developed to calculate a and b values over a grid using both the MLE and LSM methods for b values, and the LSM method for a values. The program includes data quality thresholds to determine where values can be reliably calculated, and where data is too sparse.

Earthquakes were extracted from the AGSO – Geoscience Australia database for all of Australia between January 1970 and December 2000 inclusive, and above magnitude 2.5 (generally M_L , however if other magnitudes were present instead, they are used). The magnitude 2.5 cut-off was used as this gives reasonable completeness for the main seismic

regions of Australia (although some regions may have less complete data). Aftershocks were removed so that the a and b values could be calculated for main events only (since aftershock sequences may have different characteristics). The final dataset included 5294 events. The grid used for sampling the dataset across Australia was 50 squares wide by 40 squares high (1.1 degrees wide by 0.95 degrees high, or ~105km on a side in central Australia) as this gave the best resolution of data without excessive gaps. The a and b values for a given cell (one quarter of a grid square) are the smoothed average of the data in it and the eight surrounding cells, and are normalised to 10,000km². The result for a given cell was considered valid if it was based on 15 or more events, and had a least-squares correlation coefficient (r -value) ≥ 0.6 .

Results

The contoured MLE b values are shown in Fig. 1. The majority of seismic activity in Australia occurs in the southwest seismic zone, the Adelaide Geosyncline, and in the southeast of Australia. Four other regions contained enough data to give useful results, including areas along the northwest shelf, the Kimberley in WA, central Australia, and the eastern goldfields of WA (Fig. 2A). Events in each of these seven zones were extracted from the database and used to calculate overall a and b values for each zone (without smoothing; Fig. 2B). There is little difference between the results of LSM and MLE.

Gutenberg-Richter plots of the regional data (Fig. 2B) show a strong similarity in the slope and shape of the curves for the southwest, WA goldfields, and northwest zones. A similar comparison can be made between the Adelaide Geosyncline and southeastern seismic zones. The Kimberley and central zones, however, show quite different characteristics.

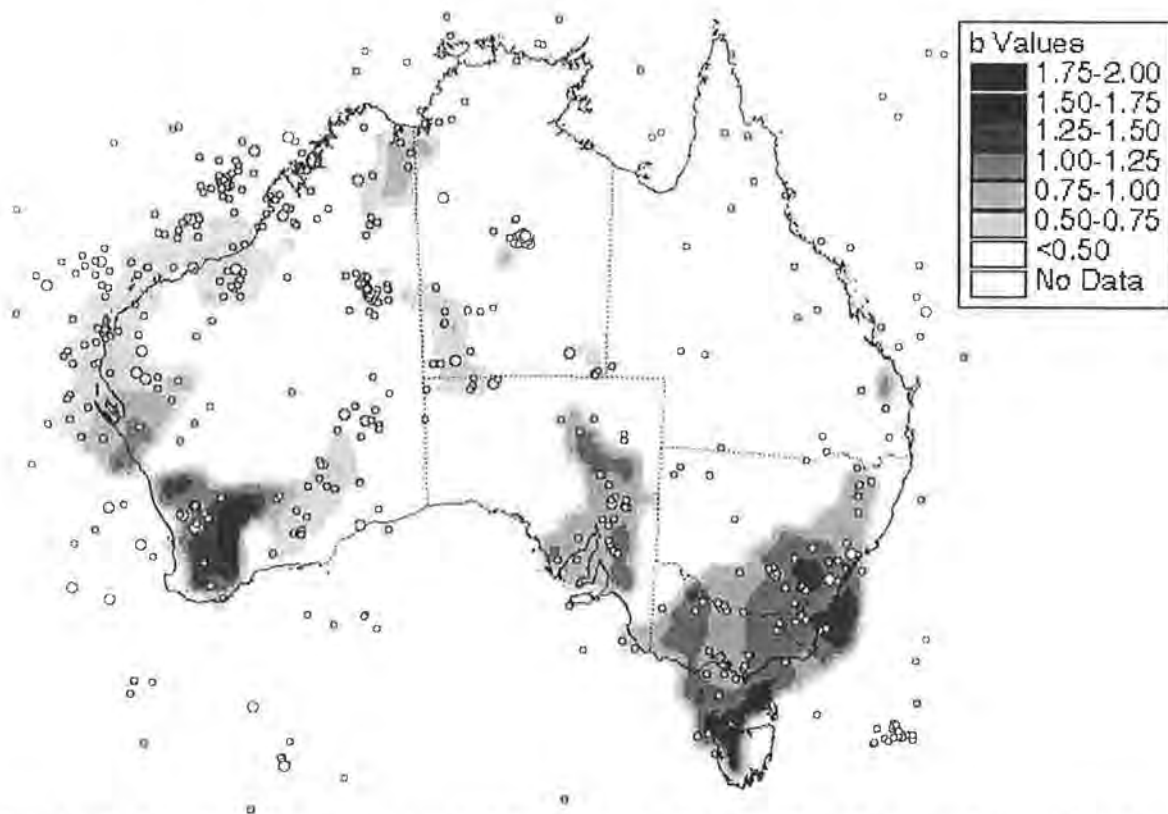


Fig. 1. Maximum likelihood estimates (MLE) of b values for Australia. Also plotted are earthquake epicentres for events of magnitude >4.0 from 1970-2000.

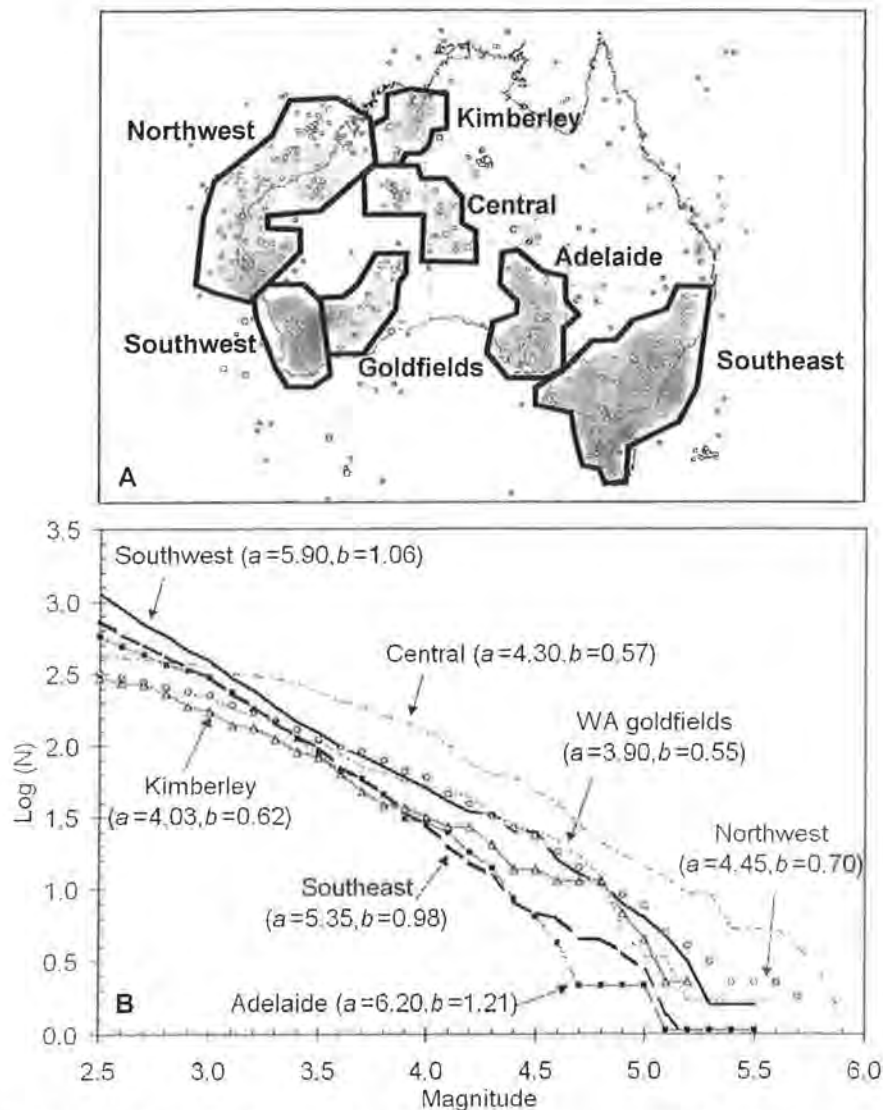


Fig. 2. A. Outlines of the seismic zones used in this study (overlain on b value contours of Fig.1), defined by areas with 15+ events per 10,000km² per 30 years. B. Cumulative number versus magnitude plots of events from each of the seismic zones used. Abrupt changes in slope near magnitude 3.0-3.5 may indicate data incompleteness. For each zone, the estimated a and b values are shown.

Discussion

This method of characterising the style of seismicity can be a useful addition to the selection of earthquake hazard assessment tools available. For instance, the areas of seismic activity outlined in Fig. 1 correspond well with the hazard areas defined by the Earthquake Hazard Map of Australia developed for the Australian Building Code (AS1170.4) based on estimated acceleration coefficients. That method described how earthquakes affect different areas based on their past characteristics. The method used in this study helps to define the style of seismicity in different areas. It gives an indication of whether a building in a certain area may experience many small earthquakes with little risk of a large event over its lifetime, or whether there is a significant chance it may be exposed to several medium to large events. The dataset used was adequate for this study, however, incompleteness of the

data does limit the usefulness of the results. Acquisition of new data from other agencies and the continual improvement of seismic networks will improve the results obtained.

Spatial Distribution of Large and Small Earthquakes

Introduction

It is widely assumed that large earthquakes are more likely to occur in areas where there have been prior small earthquakes, and many seismic hazard assessment methods assume that past seismicity is the best predictor of future seismic activity. Despite this, only recently has the premise been objectively tested. In a series of papers, Kafka and others have performed statistical analysis of this hypothesis (Kafka and Walcott, 1998; Kafka and Levin, 2000; Kafka, submitted). Their method was developed for the northeastern USA where the processes that cause earthquakes are not well understood, and was subsequently tested in several other regions of differing seismicity (including interplate and intraplate regions). Their results confirm that large earthquakes (≥ 4.0) are significantly more likely to occur in areas where there have been prior small (≥ 2.0) events. This study applied Kafka's approach to Australian earthquake data to test this hypothesis, and compare the behaviour of different seismic regions in Australia.

Methods

A program was written based on algorithms provided by Kafka (written commun., 2001). Before processing, the data is arbitrarily divided into seven year subcatalogues (after Kafka and Walcott, 1998), although future work may define optimal time frames.

For each sequential pair of subcatalogues, each large event in the later subcatalogue is compared to every small event in the previous subcatalogue. Every large event that occurred within a given radius of a prior small event is counted as a 'hit'; the large event was "predicted" by the small event. The percentage of hits is calculated, as is the percentage of the total area covered by circles of the given radius around all small events in the subcatalogue. A final run is performed in which an early subcatalogue of small events is compared to the most recent subcatalogue of large events to test the effectiveness of the method over longer time frames.

The analysis was carried out on four areas: the southwest seismic zone, the Adelaide Geosyncline, southeast Australia, and Tasmania. For each area, the analysis was carried out on the most complete data range available using radii of 5, 10, 25, 50, 75, and 100 km. Plots of the percentage of hits versus the percentage area show the likelihood that large events occur in areas where there were previous smaller events. Data plotting below the 1:1 line indicate that large events occur where there were no previous small events. Data plotting near the 1:1 line indicate that large events occur randomly and are unaffected by the occurrence of earlier small events. Data plotting above the 1:1 line indicates that large events are more likely to occur where there have been previous small earthquakes. Incomplete data would cause results to plot near or below the 1:1 line since fewer small events would be recorded and so would be less likely to predict large events.

Results

Fig. 3 shows plots of the results for each of the four areas. In all regions the results plot above the 1:1 line, indicating that large events do tend to occur where there have been previous small events. From the shape of the curves it is also possible to infer characteristics of the seismicity in that area.

The trends shown for the southwest region indicate that most large events occur within 5-10 km of prior small events, and all occur within 25-50 km of small events (except

for a couple of large events in the first run, probably due to a lack of data completeness for the small events in the earliest data), suggesting tight control of large event locations by small events. The southeast region shows a smooth distribution of large events out to 75-100 km from small events, suggesting moderate control of large event locations by small events.

The results for South Australia and Tasmania are much more erratic, and the results vary from run to run, likely due to incomplete data coverage. South Australia has some large events within 5-10 km of small events, but also has several that occur more than 100 km from small events. The Tasmanian results suggest that large events tend to occur 10-75 km from small events, but not often closer or farther.

Inferences about the characteristics of seismicity are strongly dependent on data completeness and location accuracy, and there is a problem with completeness in some areas, making the acquisition of new data crucial. Although the lack of completeness makes these inferences uncertain, it would seem that this method might be useful in characterising variations in seismicity between areas, and should be followed up using new data.

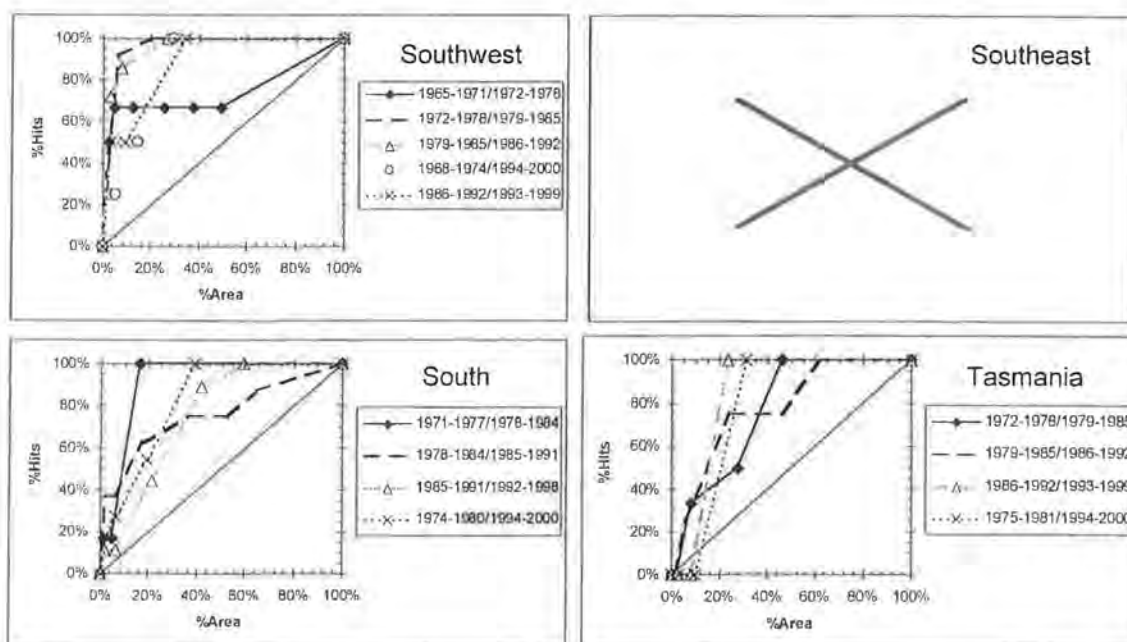


Fig. 3. Results of the Kafka analysis for the four regions in this study. Each series is a run comparing small events from the first time period to large events in the second time period, and each point represents the results at a given radius (5, 10, 25, 50, 75, and 100 km respectively along each line from lower-left to upper-right). Also shown is the 1:1 line where the percent hits = the percent area covered.

References

- Aki, K., 1965, Maximum likelihood estimate of b in the formula $\log N = a - bM$ and its confidence limits: Bulletin of the Earthquake Research Institute, Tokyo University, v. 43, p. 237-239.
- Gaull, B.A., Michael-Leiba, M.O., Rynn, J.M.W., 1990, Probabilistic earthquake risk maps of Australia: Australian Journal of Earth Sciences, v. 37, p. 169-187.
- Gutenberg, B., and Richter, C.F., 1949, Seismicity of the Earth and associated phenomena: Princeton University Press, 273p.

- Gutenberg, B., and Richter, C.F., 1944, Frequency of earthquakes in California, *Bulletin of the Seismological Society of America*, v. 34, p. 185-188.
- Kafka, A.L., submitted, The spatial distribution of seismicity in a region: To what extent does it delineate where future large earthquakes are likely to occur?: *Journal of Geophysical Research*.
- Kafka, A.L., and Levin, S.Z., 2000, Does the spatial distribution of smaller earthquakes delineate areas where larger earthquakes are likely to occur?: *Bulletin of the Seismological Society of America*, v. 90, n. 3, p. 724-738.
- Kafka, A.L., and Walcott, J.R., 1998, How well does the spatial distribution of smaller earthquakes forecast the locations of larger earthquakes in the northeastern United States?: *Seismological Research Letters*, v. 69, n. 5, p. 428-440.
- Utsu, T., 1999, Representation and analysis of the earthquake size distribution: A historical review and some new approaches, *in*, Wyss, M., Shimazaki, K., and Ito, A., [eds.], 1999, *Seismicity patterns, their statistical significance and physical meaning*: Birkhäuser Verlag, 726p.
- Weichert, D.H., 1980, Estimation of the earthquake recurrence parameters for unequal observation periods for different magnitudes: *Bulletin of the Seismological Society of America*, v. 70, p. 1337-1346.

SEISMIC PROVISIONS OF PAPUA NEW GUINEA CODE OF PRACTICE

ANIL K AGGARWAL
PNG UNIVERSITY OF TECHNOLOGY, PAPUA NEW GUINEA

AUTHOR:

Dr Aggawal is currently working as an Associate Professor in the Department of Civil Engineering at the PNG University of Technology in Lae, Papua New Guinea. He graduated from the Indian Institute of Technology, New Delhi, India in 1973 and then started his professional career as a Design Engineer, working for the Civil Construction Wing of Post and Telegraph Department. A year later he was selected, as a Scientific Officer by the Research and Development Organisation of the Ministry of Defence in India. His teaching career started in 1981, when he joined the Department of Civil Engineering at the PNG University of Technology in Lae, Papua New Guinea..

ABSTRACT:

Seismic provisions for the design of buildings in Papua New Guinea are laid down in the Earthquake Loadings Code – PNGS 1001-1982 Part 4. The Code is one part of a series dealing with general design methods and design loadings to be used for buildings in the country. It is based on the old New Zealand Standard NZS 4203 - 1976 (General Structural Design and Design Loadings for Buildings) Part 3 – Earthquake Provisions.

At the time of preparation of the PNG Code, direct adoption of other world design loading codes was considered inappropriate because most earthquake codes are aimed at high-rise buildings which do not constitute a major portion of Papua New Guinea construction. Although the seismic design procedures have increased in their degree of sophistication over the years, it is considered that the present PNG Code provides a realistic compromise in design standards on one hand and what is expected in practical design and construction on the other.

1. INTRODUCTION

Most of the seismic building codes in the world have been developed in the last 50 years, although, need for earthquake resistant structures was felt much earlier. Information on the nature of earthquake forces and the effect they have on structures was available before Codes were formulated, but it was widely scattered and not easily accessible to the designers. Moreover, the available information was insufficient to warrant legislation of design and construction procedures. Even now, response of many different types of structures to earthquake forces is not fully understood and therefore most codes of practice for seismic design, attempt to make a realistic compromise in what is known and understood on one hand and what is expected in practical design and construction on the other.

The design of earthquake-resistant structures might appear to be a straightforward application of the theory of structures and the theory of vibrations, but these theories are difficult to apply in the case of earthquakes, because of their irregular pattern and inconsistent periodicity. Looking at the transient nature of earthquakes and lack of information on loads induced, most codes of practice make simplified assumptions and rely heavily upon protective construction to reduce their adverse effects. Most countries, depending on the risk to life and property acceptable to them, define load levels which are used in the design of structures and these are reflected in their Codes. The basic philosophy of the Codes is to design structures so that human suffering and economic loss is minimised, in the event of an earthquake. The same underlying principles have been used in establishing design load levels in the Papua New Guinean Code and the basic philosophy for earthquake resistant design has been stated as:

a) in small or moderate earthquakes which occur frequently, the building should remain substantially undamaged.

b) in large earthquakes, which have a low probability of occurrence during the life of the building, the structure should have a minimal possibility of collapse but some damage is acceptable.

This philosophy while maintaining an acceptably low level of risk to public safety also ensures economically acceptable design load levels.

2. PNG EARTHQUAKE LOADINGS CODE

PNG Earthquake Loading provisions are specified in Papua New Guinea Standard - [PNGS 1001- 1982 Part 4]. The Standard is one part of a series dealing with general design methods and design loading to be used for buildings in the country. It is largely based on the old New Zealand Standard [NZS 4203 - 1976, Part 3] because seismicity of New Zealand is believed to be similar to that of Papua New Guinea.

For the purpose of building construction in Papua New Guinea, the Earthquake Loadings Standard divides the country into 4 seismic zones (Fig. 1) with the city of Rabaul (city

with 2 active volcanoes) being placed in Zone 1 (most active) and Port Moresby placed in Zone 4 (least active). The boundaries between different zones were determined from the analysis of earthquake data and the seismicity of the region. It should be noted that there are still many areas in the country for which sufficient earthquake data is not available. For such locations, designers are advised to exercise cautious judgement while designing buildings.

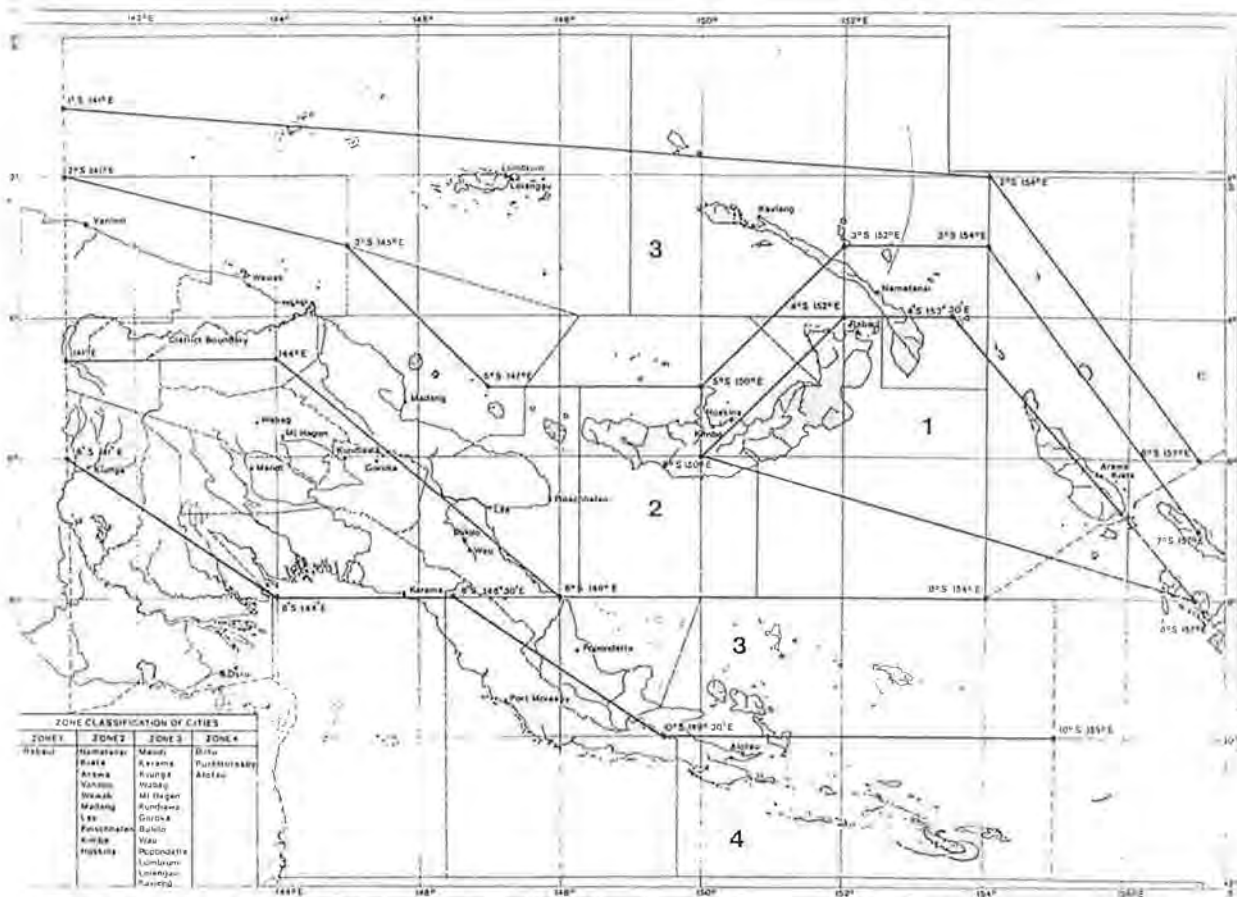


Fig. 1. Seismic Zones for Building Construction in Papua New Guinea

3. METHODS OF ANALYSIS

The PNG Earthquake Loadings Code recognises two methods for the analysis of structures:

- a) equivalent static load and
- b) dynamic analysis

For regular and simple structures up to a height of 40 m, 'equivalent static load' analysis is recommended while for all other structures, including irregular buildings and buildings with height greater than 40m, 'dynamic' analysis is mandatory.

3.1 Equivalent Static Load Analysis

The Standard recommends that all buildings designed and constructed in Papua New Guinea should withstand a total horizontal seismic base shear (V) calculated according to the following formula:

$$V = C I K W_t \quad (1)$$

where C is the basic seismic coefficient, I is the importance factor, K is structural type factor and W_t is a combination of total vertical dead and a reduced design live load above the level of lateral restraint.

It is expected that structures designed by this method will safely resist moderate earthquakes without significant structural damage. During severe earthquakes, the method relies heavily on the ability of structures to dissipate energy with inelastic deformations.

3.1.1 Basic Seismic Coefficient - C

The Code recommends that the seismic coefficient should be determined from the response spectra given for each of the 4 zones in Papua New Guinea - Fig. 2. It should be noted that the design spectra is assumed to provide a uniform risk (due to earthquake damage) in all the zones. Empirical formulae have been provided in the Standard to determine the fundamental time period of structures made from steel, concrete and other materials. In addition, two types of subsoil (firm and soft) are considered in the selection of ' C '. A definition for a 'firm' and a 'soft' soil is also provided to assist designers in the application of the Standard.

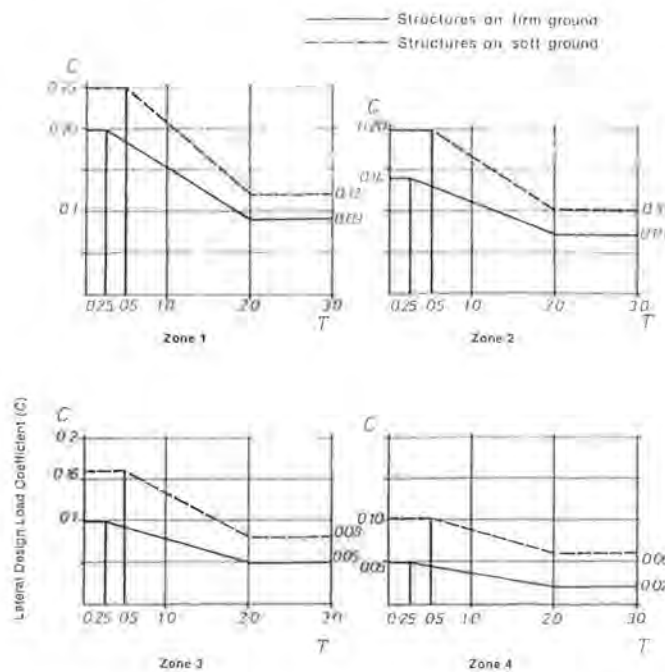


Fig. 2 Basic Seismic Coefficient C for 4 Zones in Papua New Guinea

3.1.2 Importance Factor - I

The Importance Factor is a coefficient applied to increase the return period of damage for structures of sufficient importance to warrant the additional capital expenditure. Such structures are community buildings or buildings housing services which are required to remain functional after a severe earthquake.

In the PNG Code, the factor is applied in 3 discrete values - (1.0, 1.5, 2.0) depending on the importance of the structure. Structures associated with the distribution facilities for gas or petroleum products in urban areas attract an importance factor of 2.0, while most of the other structures such hospitals, water works and power stations etc. are assigned an importance factor of 1.5.

3.1.3 Structural Type Factor - K

The Structural Type Factor is intended to reflect the potential seismic performance of different structural systems. The specified level of K primarily takes into account the ability of the structural type and construction material concerned to dissipate energy in a number of load cycles i.e. its ductility.

Ductile moment resisting frames designed and detailed according to the relevant material Standards are deemed to exhibit ductile behaviour and are assigned a structural type factor of 1.0, while structures designed and detailed with moment resistant joints and those exhibiting minimal ductility are assigned a factor of 4.0.

3.2 Dynamic Analysis

Two methods of dynamic analysis are recommended by the Code - the spectral modal analysis which is the simplest method and the numerical integration method.

3.2.1 Spectral Modal Analysis

In spectral modal analysis, the standard recommends the use of first three (3) translational modes for calculating the dynamic response of regular structures. For slightly imbalanced buildings, it is required that the response be calculated from the first five (5) modes of vibration, while for irregular and for particularly tall structures, the Code recommends that greater number of modes have to be considered, but it does not specify the exact number.

In the Code, a design spectra for spectral modal analysis has also been provided - Fig. 3. It has been determined by consideration of the spectra from actual earthquake records. For short periods, the coefficient has been adjusted to reduce the base shear to the level appropriate for a relatively high percentage of damping while for long periods, the values of the coefficient have been increased.

A 10 percent reduction in the total horizontal seismic base shear has been allowed for buildings for which modal analysis is carried out, because it is believed that more accurate distribution of the seismic base shear will result when such a reduction is applied.

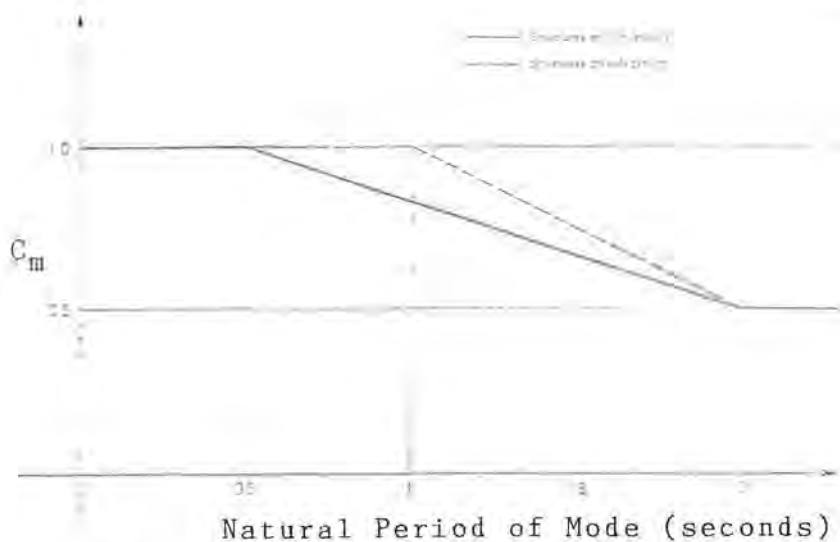


Fig. 3. Design Spectra for Spectral Modal Analysis

4.0 CONCLUSIONS

Papua New Guinea has a comprehensive Earthquake Loadings Code, even though it is not a state-of-the-art document. It takes into account the high seismic activity experienced by the country and aims to provide a realistic compromise in design standards on one hand and what is expected in practical design and construction on the other. The Standard sets load levels, such that risk to human life and property is acceptably low.

Since the publication of the Code, collapse of several engineered and non-engineered buildings has taken place, particularly in Rabaul and after the volcanic eruption of 1994. It should be noted that these failures occurred not because of the inadequacies in the design procedure, but largely due to structural roofs caving in under the heavy load of volcanic ash. In a separate study, it has been recommended that higher gravitational loads (Dead & Live Loads) should be considered for areas experiencing seismic and volcanic activities simultaneously.

5.0 REFERENCES

New Zealand Standard - NZS 4203 - 1976, Code of Practice for General Structural Design and Design Loadings for Buildings, Wellington, New Zealand, 1976

Papua New Guinea Standard - PNGS 1001 -1982, Parts 1-4, General Structural Design and Design Loadings for Buildings, National Institute of Standards and Industrial Technology, formerly National Standards Council of PNG, Port Moresby, 1982.

THE SPATIAL AUTO-CORRELATION METHOD FOR PHASE VELOCITY OF MICROSEISMS – ANOTHER METHOD FOR CHARACTERISATION OF SEDIMENTARY OVERBURDEN

MICHAEL W. ASTEN
DEPARTMENT OF EARTH SCIENCES, MONASH UNIVERSITY

AUTHOR:

Michael Asten is a consulting geophysicist and Partner with Flagstaff Geo-Consultants, and also holds an academic position as Principal Research Fellow at Monash University.

He majored in Physics, Geology and Geophysics at the University of Tasmania, and gained a PhD in geophysics from Macquarie University on the topic of using microseismic waves as a tool for studying sedimentary basins. In 1977 he took up a two-year appointment lecturing and coordinating an MSc (geophysics) programme in Nigeria. He then joined BHP Minerals in 1979 and worked in coal and base-metal exploration in Australia, East Africa and North America, with particular emphasis on geophysical research issues. He initiated a numerical modelling project in in-seam (coal) seismic modelling which became a standard tool in interpretation of commercial surveys. In the last decade he has specialised in electromagnetic and gravity exploration methodologies for mineral exploration, and is author or co-author of 70 technical papers.

He was a co-recipient of the CSIRO Medal for External Research in 2000 and co-recipient of the ASEG Graham Sands Award in 2001, (both of these for development of the "Falcon" airborne gravity gradiometer).

ABSTRACT:

The use of small circular seismic arrays rather than individual seismometers allows the method of microseismic zonation of sediment thickness and earthquake hazard to be extended, giving direct estimates of shear-wave velocity and thickness of sediments over basement. The method is well-suited to built-up areas where cultural sources of microseisms are spatially distributed, and can be extended to yield useful data where microseismic energy propagates in higher as well as fundamental modes.

1. INTRODUCTION

The use of microseisms as a tool for assessing the characteristics of sedimentary overburden has progressed down two paths over the last 50 years. The method of studying spectra as popularised by Nakamura (1989) is in common use (Jones, 2000), and has the advantages that data can be obtained using single or multiple seismometers distributed over the area of interest, recording independently. The method of measuring phase velocity of microseismic energy appears less well known outside Japan for this purpose, but has the advantage of yielding more quantitative information on sub-surface sediment and rock boundaries.

The sources and modes of propagation of microseismic energy have been studied for a century. High-frequency microseisms (above 1 Hz) are predominantly due to cultural sources (machinery, road traffic) (eg Frantti, 1963; Douze, 1967) while lower-frequency energy is attributable to wave action at coast lines and other meteorological phenomena. Most of the energy in microseisms propagates as surface waves (eg Toksoz and Lacoss, 1968; Haubrich and McCamy, 1969). Surface-wave energy can propagate in a fundamental and also in higher modes, each mode having its own phase-velocity dispersion curve. Reviews oriented to this topic are available in Asten (1976, 1978b) and Okada (1997). The book by Okada (1997) also provides detailed studies of the spatial and temporal variations in high-frequency microseismic energy.

It is the purpose of this paper to summarise some results from the latter method, and thus illustrate how it may be applied to engineering studies such as earthquake hazard zonation tasks in Australia.

2. INFORMATION CONTENT IN MICROSEISMS

In this paper we consider only vertical-component microseismic energy, which limits interpretation to consideration of Rayleigh-wave energy only. The microseismic spectral method for zonation relies on detection of peaks in spectra which are associated with resonances. Compressional-wave resonances are closely associated with surface-wave group-velocity minima (Mooney and Bolt, 1966)

The phase-velocity dispersion method relies on measuring changes in phase velocity with frequency; high-frequency surface waves have shallow penetration; low frequency waves have deeper penetration into more consolidated sediments, and hence are faster. The maximum sensitivity of velocity to depth to an interface, occurs at frequencies where the dispersion curve dC/df changes most rapidly with frequency. These frequencies (by definition) correspond with the frequencies of minima in the group velocity.

The reason the spectral and phase velocity methods yield similar information is that a point force on an elastic medium produces a motion spectrum inversely proportional to the mean energy flux, where minima in the energy flux are closely associated with group velocity minima (Hudson and Douglas, 1975). Thus the two techniques measure closely related phenomena. The phase velocity has the advantage however that it is an absolute measurement which can in principle be inverted to yield profiles of shear velocity vs depth. Where for example Turnbull (2000) computed shear-velocities for surficial sediments from Standard Penetration Tests using an empirical relation from another area, actual measurement

of phase velocity of microseisms at selected sites would yield direct shear-velocity estimates for each site surveyed.

3. MEASUREMENT OF PHASE VELOCITY

The variation of phase velocity with frequency can be measured using array-processing methods. Two generic approaches are possible. The best known is frequency-wavenumber beam forming (Capon, 1969) which yields both wave velocity and direction to the source. This method however suffers from biases in velocity estimates when multiple sources interfere. An alternative approach is the spatial auto-correlation method (SPAC) which has the significant advantage that it extracts scalar wave velocity irrespective of direction to the source.

The SPAC method applied to the study of near-surface geology has had a fascinating history over the last 50 years. Aki (1957, 1965) laid the foundation, but his contribution appears to have been largely ignored in Western literature on the study of microseisms, apart from Asten (1976, 1978a, 1983); the great strides in seismic array data processing of the 1960s and 1970s were spurred by the need to locate *direction* to seismic sources, and hence beam-forming methods (eg Capon, 1969) received the greatest emphasis. Okada (1997) summarises developments and comparisons of the SPAC method and beam-forming methods in Japan, from the last decade.

The SPAC technique is worthy of an additional observation. Whereas array beam-forming delivers estimates of wave velocity and direction, and is subject to bias in velocity estimates when waves from multiple directions are incompletely resolved, the SPAC technique has the delightful property that, since the wave direction is not sought, estimates of wave scalar velocity are unaffected by the super-position of waves from multiple directions (Aki, 1965; a principle subsequently overlooked in some literature, eg Douze and Laster (1979), but then reiterated by Asten, 1983). In fact, the more omni-directional the wave energy (assuming single-mode propagation), the better the estimate of scalar velocity. The SPAC technique thus has the serendipitous property of giving its best results when seismic sources are many. This is why the technique has enormous potential in built-up areas, where microseismic noise militates against the use of conventional seismic methods, but that same ubiquitous noise generated by urban activity produces an omni-directional wave-field of high-frequency microseisms, ideally suited to the SPAC technique.

4. THE SPAC METHOD FOR SINGLE AND DUAL MODE WAVE PROPAGATION

The coherency $c(f,r,\phi)$ at angular frequency f , between two stations separated by distance r , azimuth ϕ , sampling a single propagating plane wave may be written

$$c(f,r,\phi) = \delta(f-f_0) \exp(i k_0 r \cos \phi) \quad - (1)$$

where δ is the delta function, and k_0 is the wavenumber.

If we use a circular array of seismometers, compute coherency over a range of azimuths, and azimuthally average the coherencies, the integration of equ (1) with respect to ϕ yields

$$\overline{c}(f,r) = \delta(f-f_0) J_0(k_0 r) \quad - (2)$$

$$= \delta(f-f_0) J_0(2 \pi f r / C(f)) \quad - (3),$$

where $C(f)$ is the scalar phase velocity at frequency f .

If the wave energy is confined to a single mode and velocity at frequency f , then computation of $c(f,r)$ at a range of discrete frequencies allows the phase velocity $C(f)$ at those frequencies to be computed by direct solution of equ (3). Derivation of this result is given with greater rigour by Aki (1957, 1965) and Okada (1997).

If the propagating energy consists of multiple modes (velocities) at a given frequency, the coherencies are degraded and velocity estimates will be in error. This is a potential problem since surface waves do propagate in multiple harmonic modes. However from Asten (1976) we may extend equ (3) by making an assumption that energy at frequency f is confined to two modes with energy fractions p and $(1-p)$ having wavenumbers k_0 and k_1 respectively. The three unknowns k_0 , k_1 and p can be solved if we have coherency measurement simultaneously over three (or more) seismometer separation distances r_1 , r_2 and r_3 . A circular array of radius r , with six circumferential and one central seismometer, allows sampling of the wave field over three distances, r , $1.7r$, and $2r$, and hence the SPAC method can solve for dual velocity modes.

Okada (1997) develops another extension of the SPAC method, for estimation of the velocity of microseismic energy propagating with horizontal-component motion, hence in principle the method can also be used to obtain velocity dispersion curves for Love-wave microseismic energy.

5. EXAMPLE - COASTAL PLAIN, JAPAN

Matsuoka et al (1996) provide an example (Figure 1) showing the results of single-mode SPAC method at four locations on the coast of Japan. Drilling, acoustic logging and refraction seismic observations on the sediments provide shear velocity profiles which are used to compute fundamental-mode Rayleigh-wave dispersion curves. The computed curves (solid lines) and velocity estimates from the SPAC method (symbols) show a close correspondence. Note that four triangular arrays with radii from 3 to 121 m were used to give resolution over a wide range of wavenumbers.

These results suggest that inversion of the observed dispersion curves should be able to provide independent means of estimating the shear-velocity profile of the sediments without recourse to drilling. Okada (1997) provides further case histories where this inversion step has been applied to the phase-velocity data.

6. EXAMPLE – SYDNEY BASIN

Asten (1976) acquired microseismic data using a seven-station circular array of radius 50 m, on Quaternary sediments near Richmond (NSW) near the centre of the Sydney Basin. The velocity structure was independently established from a refraction seismic survey (to 50 m depth) and petroleum exploration (to 3 km). Figure 2 shows phase velocity estimates from microseisms recorded with the array, over a single 20 sec data length. Three techniques are demonstrated for extraction of phase velocities; frequency-wavenumber beam-forming, the single-mode SPAC method, and the dual-mode SPAC method. The beam-forming method indicates that wave propagation is dominated by fundamental modes at high frequencies (6-10 Hz) and the 1st higher mode at frequencies 2.5-5 Hz. The single-mode SPAC method gives a less scattered dispersion curve with velocities falling between the fundamental and higher-mode curves. The dual-mode SPAC method yields pairs of velocities which correlate

well with the two modes; the majority of the energy (square symbols) lies on the fundamental-mode curve at high frequencies, and on the higher mode at lower frequencies, thus confirming the indication provided from beam forming, but also providing the additional resolution of the two modes. Further details are given in Asten (1976).

7. CONCLUSIONS

The SPAC method of processing data from small circular arrays of seismometers is capable of resolving information on thickness of sediments and, most importantly, the shear-velocity profile for those sediments. The method uses microseismic energy generated by multiple natural and cultural sources, and is suitable for use in built-up areas.

I see scope for several further developments in the use of microseisms for engineering and environmental zonation of areas of sedimentary fill, in built-up localities. Firstly, the integrated study of both spectral shapes and phase velocities is likely to provide more information than either discipline alone. Secondly, the extension of the SPAC technique to dual-mode propagation may extend the utility of the methodology currently in routine use in Japan. Thirdly, the routine use of three-component seismometers with the horizontal-mode SPAC method outlined by Okada (1997) should allow simultaneous detection and use of both Rayleigh and Love-wave microseismic energy.

8. REFERENCES

- Aki, K. (1957) Space and time spectra of stationary stochastic waves, with special reference to microtremors. *Bull. Earthq. Res. Inst.*, Vol 35, pp 415-456.
- Aki, K. (1965) A note on the use of microseisms in determining the shallow structures of the earth's crust. *Geophysics*, Vol 30, pp 665-666.
- Asten M.W. (1976) The use of microseisms in geophysical exploration: PhD Thesis, Macquarie University.
- Asten M.W. (1978a) Phase velocities of mixed-mode high-frequency microseisms" (Abstract): *EOS*, Vol 59, No.12, p 1141.
- Asten M.W. (1978b) Geological Control on the Three-Component Spectra of Rayleigh-wave Microseisms. *Bull. Seism. Soc. Am.*, Vol 68, pp 1623-1636.
- Asten M.W. (1983) Discussion on 'Seismic Array Noise Studies at Roosevelt Hot Springs, Utah Geothermal Area'. *Geophysics*, Vol 48, pp 1560-1561.
- Capon, J. (1969) High-resolution frequency-wavenumber spectrum analysis. *Proc. IEEE*, Vol 57, pp 1408-1418.
- Douze, E.J. (1967) Short period seismic noise. *Bull. Seism. Soc. Am.* Vol 57, pp55-81.
- Douze, E.J. and Laster, S.J. (1979) Seismic array noise studies at Roosevelt Hot Springs, Utah Geothermal Area. *Geophysics*, Vol 44, pp 1570-1583.
- Frantti, G.E. (1963) The nature of high-frequency earth noise spectra. *Geophysics*, Vol 28, pp547-562.
- Haubrich R.A. and McCamy, K. (1969) Microseisms: Coastal and pelagic sources. *Rev. of Geophys.* Vol 7, pp 539-571.
- Hudson, J.A. and Douglas, A. (1975) Rayleigh wave spectra and group velocity minima, and the resonance of P waves in layered structures. *Geophys. Jour. Roy. Astr. Soc.* Vol 42, pp 175-188.
- Jones, T. (2000) Earthquake Risks, in *Community risk in Mackay: a multi-hazard risk assessment*, M. Middelman and K. Granger (eds), AGSO-Geoscience Australia.
- Nakamura, Y. (1989) A method for dynamic characteristics estimation of subsurface using microtremors on the ground surface: Quarterly reports of the Railway Technical Research Institute Tokyo, Vol 30, pp 25-33.
- Konno, K. and Ohmachi, T. (1998) Ground-motion characteristics estimated from spectral ratio between horizontal and vertical components of microtremor. *Bull. Seism. Soc. Am.* Vol 88, pp 228-241.
- Matsuoka, T., Umezawa, N., and Makishima, H. (1996) Experimental studies on the applicability of the spatial autocorrelation method for estimation of geological structures using microtremors. (in Japanese with English abstract), *Butsuri Tansa*, Vol 49, pp 26-41.

Mooney, H.M., and Bolt, B.A. (1966) Dispersive characteristics of the first three Rayleigh modes for a single surface layer. *Bull. Seism. Soc. Am.*, Vol 56, pp 43-67.

Okada, H. (1997) *The Microseismic Survey Method*: Society of Exploration Geophysicists of Japan. Translated by Koya Suto, in review as Course Notes Series, Vol 12, Society of Exploration Geophysicists, Tulsa.

Toksoz, M.N. and Lacoss, R.T. (1968) Microseisms: mode structures and sources. *Science* Vol 159 pp 872-873.

Turnbull, M.L. (2000) Microzonation of Bundaberg City. Dams faults and scarps, Proceedings of a Conference held by the Aust. Earthqu. Eng. Soc., Hobart, Paper 10.

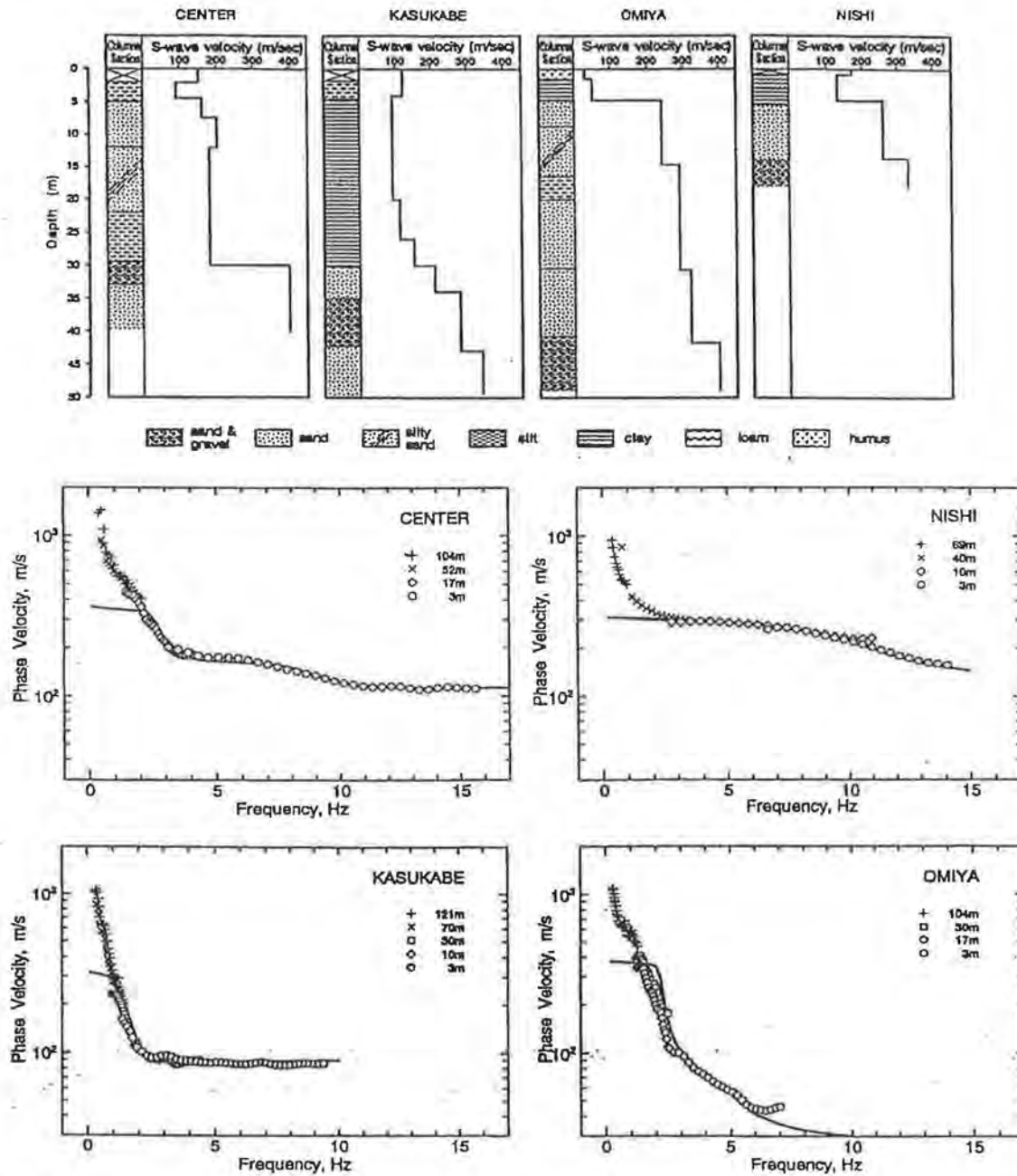


Fig. 1. Top: Detailed distribution of shear-wave velocity to the depth of 50 m, from well-log and refraction seismic surveys. Bottom: Phase velocities (symbols) of fundamental-mode Rayleigh waves, calculated from microseismic data by the SPAC method. The solid line shows phase velocities from theoretical calculations using the velocity-depth profiles above. (From Matsuoka et al, 1996; figure reproduced from Okada, 1997).

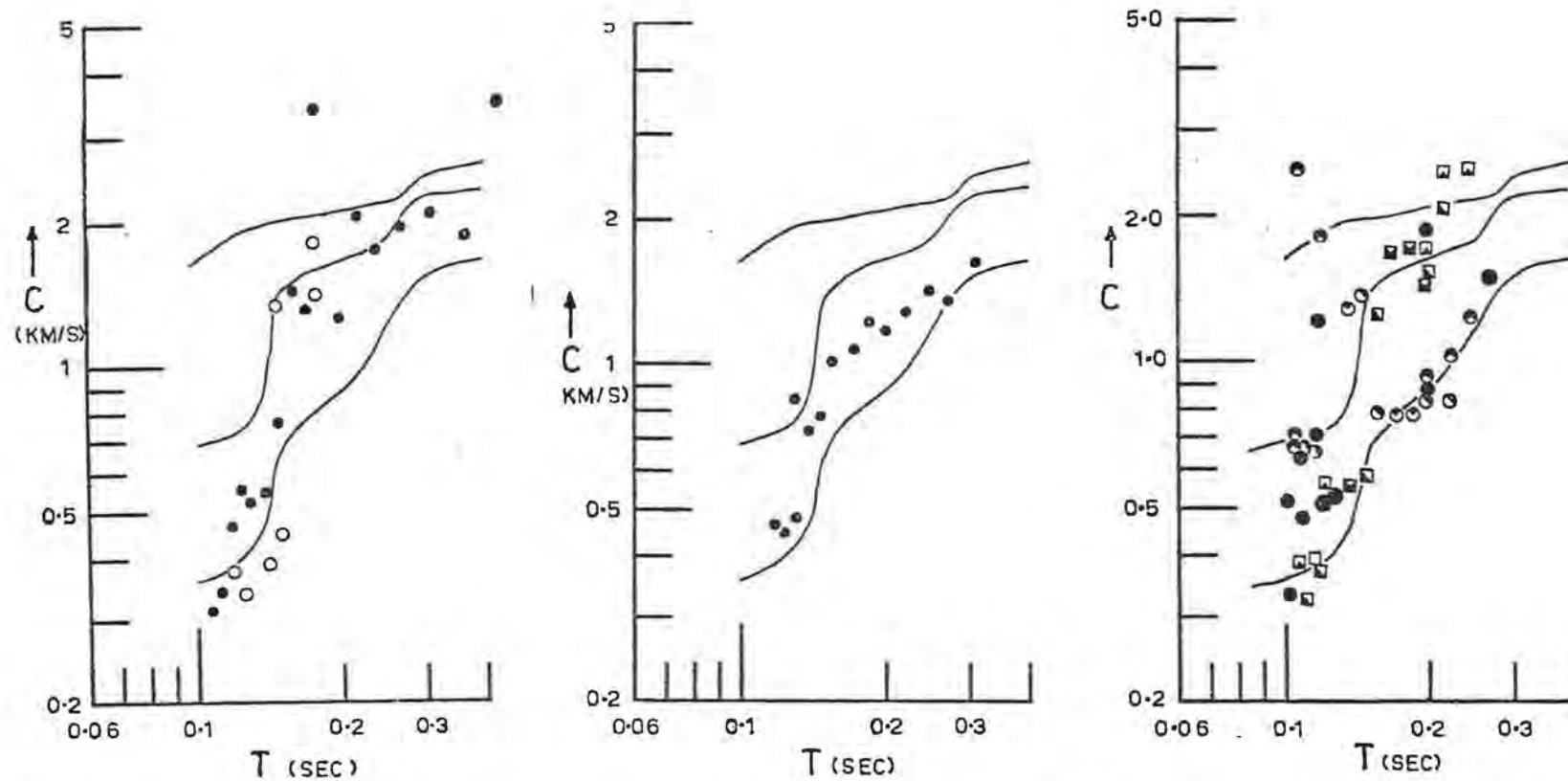


Fig. 2. Phase-velocity vs period estimates of dispersion curves, obtained using three algorithms applied to the same 20-sec length of microseismic data, acquired with a circular array of radius 50 m, with seven vertical seismometers, one at the array centre, and six on the circumference.

Left: High-resolution beam forming.

Centre: Single-mode SPAC method.

Right: Dual-mode SPAC method. Square symbols denote the dominant energy fraction (>50%).

Solid lines are theoretical dispersion curves for the fundamental, 1st and 2nd higher Rayleigh modes, computed for a 7-layered earth having compressional (α) and shear (β) velocities, thicknesses (d) and densities (ρ) as follows:

α : 300, 710, 1700, 3480, 3880, 4630, 6040 m/s. β : 150, 390, 390, 1880, 2230, 2680, 3490 m/s.

d : 1.5, 18.3, 8.5, 500, 1000, 1800 m. ρ : 1.8, 2.0, 2.2, 2.4, 2.5, 2.6, 2.8 t/m³.